IEEE Access
Multidisciplinary | Rapid Review | Open Access Journal

Received February 18, 2019, accepted March 18, 2019, date of current version April 26, 2019.

Digital Object Identifier 10.1109/ACCESS.2019.2908558

Supercapacitors: Electrical Characteristics, Modeling, Applications, and Future Trends

ALBERTO BERRUETA[1], (Member, IEEE), ALFREDO URSÚA[1], (Member, IEEE), IDOIA SAN MARTÍN[1], ALI EFTEKHARI[2], AND PABLO SANCHIS[1], (Senior Member, IEEE)

[1]Department of Electrical, Electronic and Communication Engineering, Institute of Smart Cities, Public University of Navarre, Campus de Arrosadía, 31006 Pamplona, Spain
[2]Belfast Academy, Belfast BT3 9FG, U.K.

Corresponding author: Pablo Sanchis (pablo.sanchis@unavarra.es)

This work was supported in part by the Spanish State Research Agency (AEI) and FEDER–UE under Grant DPI2016-80641-R and Grant DPI2016-80642-R, in part by the Government of Navarre through the Research Project PI020 RENEWABLE-STORAGE, and in part by the FPU Program of the Spanish Ministry of Education, Culture and Sport under Grant FPU13 /00542.

ABSTRACT Energy storage systems are playing an increasingly important role in a variety of applications, such as electric vehicles or grid-connected systems. In this context, supercapacitors (SCs) are gaining ground due to their high power density, good performance, and long maintenance-free lifetime. For this reason, SCs are a hot research topic, and several papers are being published on material engineering, performance characterization, modeling. and post-mortem analysis. A compilation of the most important millstones on this topic is essential to keep researchers on related fields updated about new potentials of this technology. This review paper covers recent research aspects and applications of SCs, highlighting the relationship between material properties and electrical characteristics. It begins with an explanation of the energy storage mechanisms and materials used by SCs. Based on these materials, the SCs are classified, their key features are summarized, and their electrochemical characteristics are related to electrical performance. Given the high interest in system modeling and a large number of papers published on this topic, modeling techniques are classified, explained, and compared, addressing their strengths and weaknesses, and the experimental techniques used to measure the modeled properties are described. Finally, SCs are successfully used in the market sectors, as well as their growth expectations are analyzed. The analysis presented herein gives the account of the expansion that the SC market is currently undergoing and identifies the most promising research trends on this field.

INDEX TERMS Electrical performance, electrochemistry, energy storage, experimental characterization, modeling, supercapacitor.

I. INTRODUCTION

The concern about climate change, the drawbacks that petroleum dependency has for many countries, and an increasingly interconnected society entail significant changes in systems. Particularly, as a result of the expansion of renewable energy generation, the electrification of the transport sector and the growing demand for wireless electrical devices, electrical energy storage systems (ESS) are growing into a major research topic [1].

Supercapacitors (SCs) are ESSs that bridge the gap between batteries and conventional capacitors with regard to energy and power densities. As shown in the Ragone Plot (Fig. 1), their specific energy is far higher than conventional capacitors and their specific power is greater than existing batteries. Li-ion batteries are suitable for applications requiring charge–discharge cycles of a few hours (for instance PV self-consumption) and traditional capacitors have optimal performance with cycle times in the order of ms or μs (e.g. power converters). In this context SCs arise as the best option for several applications in which charge–discharge cycle times ranging from a few seconds to several minutes are required, as detailed along the following sections. A number of terms are used by researchers, manufacturers and users to refer to SCs. Some authors call them electrochemical capacitors (ECs) [2] or electric double-layer capacitors (EDLC) [3], given that an electric field created in the double layer between the electrodes and the electrolyte is the primary

The associate editor coordinating the review of this manuscript and approving it for publication was Hua Bai.

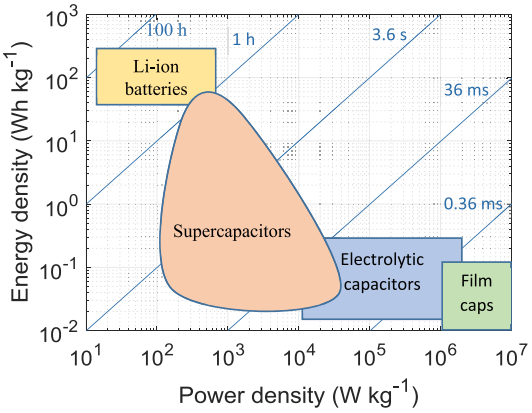

FIGURE 1. Ragone Plot of electrical energy storage systems. Characteristic times correspond to lines with unity slope.

TABLE 1. Recently-published review papers on supercapacitors.

Year	Topic	Reference
2014	Physical principles	[6]
2016	Physical principles, electrode and electrolyte materials	[7]
2015	Electrolyte materials	[8]
2016	Materials, energy storage mechanisms, characterisation and applications	[9]
2015	Electrical performance	[10]
2018	Modelling, control and applications	[11]
2019	Design, fabrication and applications of hybrid SCs	[12]

energy-storage mechanism. Since SCs behave similarly to capacitors and are often used to manage high power peaks, other authors call them pseudocapacitors or power capacitors. Ultracapacitors [4] and gold capacitors are also names used to refer to SCs. This terminology has its origin in the first commercially available SCs, launched in the late 70s and early 80s by companies such as the Nippon Electric Company (under the name ''super capacitor''), Panasonic (commercial name ''gold capacitor'') and the Pinnacle Research Institute (''PRI Ultracapacitor'') [5]. A simple bibliographic search reveals that supercapacitors is the most common name.

In recent years, numerous research papers have been published on different SC-related topics, given the evident current need for such a technology, the year-on-year market growth, the growth expectations for the future and the predicted impressive improvement potential [13]. Many review papers have been published directed at meeting the need to organize and summaries new published research findings in each field related to SCs. Table 1 summarizes the focus topic of the main recently-published review papers concerning SCs. With this work we aim to complement these SC reviews from an energy application point of view, with special focus on large scale systems. For this purpose, the relationship between the SC material properties and their electrical performance is explained using electrochemical principles. After this, the applications where SCs can play a significant role are identified, leading to an intensive analysis of the use of SC in large scale systems.

With this purpose, the information is structured into the following sections. Following this introduction, the principles of SC performance are covered in Section II, along with a summary of the most important material characteristics, a classification of SCs based on this information and guidelines for the most suitable SC type based on application requirements. In Section III, the basic electrical phenomena that can be measured in an SC are explained based on the previously-described principles. This is followed in Section IV by a description of the main trends in SC modeling, as suitable tools to relate electrochemical principles with electrical performance. This section also includes a critical analysis of the suitability of each type of model from different points of view (SC design, manufacturing, design of an energy system, storage system control strategy, etc.). Furthermore, the most commonly-used experiments to characterize the parameters of each type of model are covered, with an emphasis on their strengths and weaknesses in identifying each phenomenon. Section V goes on to analyses the key features of currently available SCs and their suitability for each type of energy system. Furthermore, we present a critical analysis of successful and recently-emerged energy applications in which SCs play a primary role as an ESS, with particular emphasis on future trends. The paper concludes with Section VI, which contains a summary of the most important aspects covered by the review, emphasizing their relevance and prospects based on the information provided herein.

II. FUNDAMENTALS AND TYPES OF SUPERCAPACITORS

The aim of this section is to explain the electrochemical mechanisms and the materials involved in SC energy storage process. Given the fact that there are similarities between the SC charge storage and the battery and capacitor operating principles, for the sake of clarity, a comparison is made with the principles explained in Section I. Furthermore, since the energy is stored on the electrode-electrolyte interfaces, the storage mechanism on each SC electrode needs to be addressed separately. A combined analysis can lead to misinterpretations when the two electrodes in a device are made of different materials. With this aim in mind, the operation principle of SCs is briefly covered in subsection II-A and the energy storage mechanisms used on each of the electrode–electrolyte interfaces are addressed in subsection II-B. Subsequently, in subsection II-C, a classification of the SCs based on *both* electrodes is presented; and a classification based on electrolyte materials is addressed in subsection II-D. Finally, the interaction between the electrodes and the electrolyte of an SC is analyzed in subsection II-E, summarizing the most noteworthy theoretical and experimental studies on this topic.

A. OPERATION PRINCIPLE

SCs consist in two porous electrodes immersed in an electrolyte. The energy is stored using the electric field created between the electrodes and the electrolyte, as shown in Fig. 2.

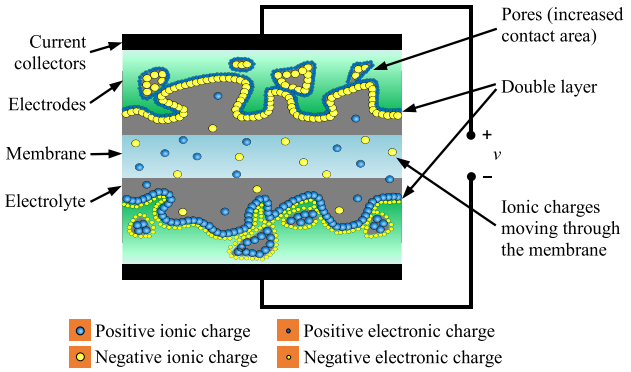

FIGURE 2. Operation principle of an SC cell.

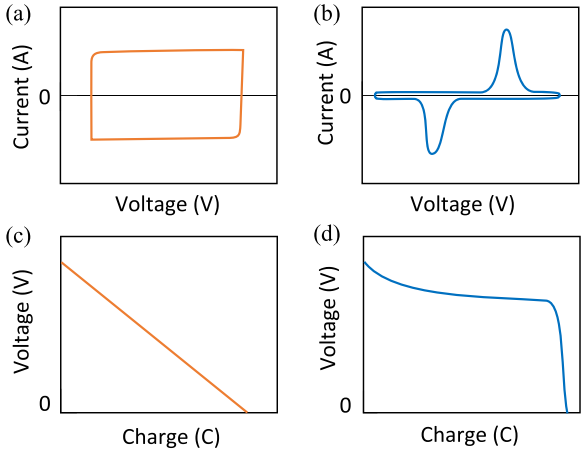

FIGURE 3. Schematic representation of cyclic voltammograms (a and b) and galvanostatic discharges (c and d). Both tests show the difference between capacitor-like behavior, typical of double-layer and pseudocapacitive mechanisms (represented in orange in graphs a and c) and battery-like (or faradaic) behavior (represented in blue in graphs b and d).

Positive charges are colored in blue and negative charges, in yellow. Ionic charges are represented bigger than electronic ones, since their size is important for the SC performance, as detailed below. Both electrodes are separated by an ion-conductive membrane, which is the central part of the schematic shown in the figure, that allows ion throughput while preventing short circuits between the electrodes.

B. ENERGY STORAGE MECHANISMS

A wide range of materials are used to manufacture SC electrodes and electrolytes, thereby determining the energy storage mechanisms occurring in the SC. A knowledge of these processes is critical for the understanding and optimal utilization of SCs. Two main experiments are performed to characterize an SC electrode, and these are convenient tools to understand the different energy storage mechanisms. On the one hand, cyclic voltammetry (see Fig. 3 (a) and (b)) is an experiment in which the electrode potential is ramped linearly versus time. When a set potential is reached, it is ramped in the opposite direction to return to the initial potential. The current is measured and plotted against the applied voltage to give the cyclic voltammogram trace. On the other hand, a galvanostatic discharge consists in a constant-current discharge of an electrode. The voltage is measured and plotted against the electrode charge (see Fig. 3 (c) and (d)). The three basic types of behavior that SC electrodes can exhibit are explained hereafter. Their properties are compared and contrasted, and the electrical performance of each type of electrode is described based on their cyclic voltammetry and galvanostatic discharge.

1) DOUBLE-LAYER BEHAVIOR

The double layer effect consists in an accumulation of two types of charge on the electrode–electrolyte interface, and is the primary storage mechanism in electrodes made of carbon powders, fibers or felts. On the one hand, an excess or a deficit of conduction-band electrons in the electrode, at or in the near-surface region of the interface. On the other hand, counterbalancing charge densities of accumulated cations or anions of the electrolyte on the solution side of the double layers at the electrode interfaces [14]. Given that the surface density of these charges, *electrostatically stored* at the electrodes interfaces, depends on the applied voltage, the double-layer capacitance varies with the electrode voltage. The only electrochemical reaction involved in double-layer behavior takes place at the surface of the electrode and consists in the adsorption and desorption of cations and anions [9]. Therefore, double-layer capacitance is characterized by rectangular cyclic voltammograms, as shown in Fig. 3 (a), since the response to a linear change in voltage is a constant current. Moreover, the galvanostatic discharge for this kind of material is linear (Fig. 3 (c)) [15].

The double layer effect takes place on every interface between electronic-conductor and ionic-conductor materials, which is a typical scenario in most electrochemical ESSs. It is, however, a parasitic effect instead of the primary energy storage mechanism in systems such as electrolyzers, fuel cells and batteries [16]–[19]. Conversely, the SC operating principle is based on this property, and its electrodes are designed with the aim of maximizing this effect.

2) PSEUDOCAPACITIVE BEHAVIOR

Pseudocapacitance is the result of fast and reversible faradaic charge-storage mechanisms [20]. Although there are similarities between these reactions and battery behavior since they involve the passage of charge across the double layer, unlike normal batteries, the capacitance is the result of a particular thermodynamic relationship between the extent of charge acceptance and the change of voltage [14]. Pseudocapacitive electrodes present a capacitor-like behavior, since their cyclic voltammogram is similar to the double layer rectangular shape (Fig. 3 (a)) and they have a linear galvanostatic discharge (Fig. 3 (c)). In comparison with double-layer electrodes, pseudocapacitive electrodes can deliver a significantly higher specific capacitance, which makes them attractive for applications requiring high energy density.

However, they suffer from two main drawbacks associated with the electrochemical reactions involved: lower power density and weaker cyclability. The reasons for these drawbacks are irreversibility and the dynamics of the electrochemical reactions involved. The irreversibilities induce a faster ageing of the electrode while the reaction dynamics limit its power capability.

The birth of pseudocapacitive electrodes is due to the discovery of the unusual electrochemical behavior of RuO_2 [21]. Since then, various cheap metal oxides have been studied as potential electroactive materials for pseudocapacitors [14], [22]. Among the currently-researched metal-oxide materials, iron based oxides and hydroxides are receiving tremendous interest due to their abundance, high specific capacitance and low toxicity [23]. Both single oxides/hydroxides such as Fe_2O_3 or FeOOH and binary metal oxides such as MFe_2O_4 or FeOOH (with M=Ni, Co, Sn, Mn, Cu, etc.) are currently being researched [24], [25] with the aim of obtaining cheap materials with suitable pseudocapacitive properties.

In addition to metal oxides, metal carbides [26] and conducting polymers [27] intrinsically display pseudocapacitive behavior. The main drawback of conducting polymers compared to inorganic materials is that, even though both have void volume to allow for the intercalation of ions, the spaces of conducting polymers are not big enough to host the ions and the intercalation causes severe volume changes in the electrode. Polyaniline (PANI) is one of the pioneering conductive materials. PANI SCs were first manufactured several decades ago, but no further research was developed due to the problems caused by volume change. Greater attention has been paid to this material over the last few years due to technology advances that have made it possible to combine PANI with other electroactive materials to enhance the electrochemical performance of SCs [28], [29].

It should be taken into account that the majority of SC electrodes available marginally fall within the pseudocapacitive category due to the presence of functional groups resulting in the occurrence of a pseudocapacitive secondary response [30]. In fact, the electrochemical response of double layer capacitors composed of nanomaterials such as graphene, is partially due to the electrochemical redox systems of electrochemically active groups over the carbon chemical and structural irregularities [31].

3) FARADAIC BEHAVIOR

This storage mechanism is based on the redox reactions of metal ions *within* the crystalline structure of the electrode. Usually, metal cations are intercalated and deintercalated, and this process needs to be coupled with redox reactions involving the electron gain or loss of the electrode material. It should be noted that this mechanism also involves phase transformation and/or alloying reactions, in addition to the passage of charge mentioned in the pseudocapacitive behavior. The electrode voltage is determined by some singular value by the Gibbs energies of pure, well-defined phases, and usually also the composition and concentration of the solution. Therefore, these materials exhibit a voltage plateau in a galvanostatic discharge (Fig. 3 (d)) and faradaic redox peaks in cyclic voltammograms (Fig. 3 (b)). The capacity[1] achieved in Faradaic electrodes is several times (10–100 times) higher than that of capacitive electrodes.

Unfortunately, many battery-type electrodes, such as $Ni(OH)_2$ or other materials, that exhibit faradaic behavior have been considered as pseudocapacitive materials in many reports, causing confusion for readers [9]. Even if the redox properties of battery materials are electrochemically reversible, they are much worse than those of pseudocapacitor materials and their charge and discharge power is limited by the ion diffusion within the crystalline framework.

It is noteworthy that the same electroactive materials can deliver either pseudocapacitive or battery-like behavior. This issue is due to the various lattice structures and nanoarchitectures that can be achieved in the electroactive material during its manufacturing process. For instance, the current applied during the electrodeposition of manganese oxide can be adjusted in order to prepare either a battery-like electrode [32] or a pseudocapacitive electrode [33].

C. TYPES OF SCS BASED ON THEIR ELECTRODES

The most suitable supercapacitor for a system depends on the specific requirements of each application. A classification of SCs highlighting their characteristic properties is a useful tool to correctly select the best SC to be used in each application. This classification based on the electrode material is the one most commonly used to categorize SCs, and it is presented herein with the aim of clarifying the different options available, identifying their advantages and disadvantages, and addressing the critical parameters and characteristics to make a rational selection of SC.

It is important to highlight the fact that the macroscopic behavior of a given device does not presume the processes that occur at each electrode inside the device, and furthermore does not indicate whether individual electrodes are capacitive or faradaic in nature. For instance, an SC formed by a faradaic electrode and a complementary capacitive electrode results in a charge/discharge plot which looks capacitive because it is the combination of a capacitive electrode (triangular shape) and a faradaic one (plateau shape).

As detailed below, SCs can be classified into three main groups: symmetric, asymmetric and hybrid SCs. Confusion sometimes arises from this classification since some authors consider hybrid SCs to be a sub-category of asymmetric SCs. Given the significant difference between hybrid SCs and the other two types of SCs regarding characteristics and performance, and following the criteria established in previous papers [9], [20], three categories of SCs are presented herein. Typical characteristics of each type of SC are summarized in Table 2.

[1]Note that *capacity* (C or Ah) and not *capacitance* (F) is the most meaningful metric for the analysis of faradaic materials.

TABLE 2. Key features of the main supercapacitor technologies.

	Symmetric	Asymmetric	Hybrid
Main storage mechanisms	Double layer	Double layer + pseudocapacitance	Double layer + faradaic
Energy density	5 Wh kg^{-1}	30 Wh kg^{-1}	100 Wh kg^{-1}
Power density	9 kW kg^{-1}	5 kW kg^{-1}	4 kW kg^{-1}
Operating temperature	–40 / 80 °C	–25 / 60 °C	–40 / 60 °C
Typical electrodes	Carbon materials	Carbon, metal oxides, conducting polymers	Carbon, intercalation materials
Typical electrolyte	Organic	Aqueous	Organic
Applicability	Commercial	Material research and early commercial	Manufacturing research and commercial
Advantages	Power density, maturity, efficiency	Trade-off energy and power	Energy density
Disadvantages	Energy density	Price, efficiency, lifetime	Power density

- Symmetric SCs: The same double-layer material is used for both electrodes. These are the most commonly used SCs, given the lower cost of the electrodes (typically activated carbon) and their higher maturity [34]. Research in these SCs is aimed at taking advantage of carbon nanotubes [35], [36], carbon aerogels [37], [38] and graphene [39]. Their energy density is relatively low, around 5 Wh kg^{-1}, and their power density is as high as 9 kW kg^{-1} [40]. Symmetric SCs are the most suitable option for energy applications in which safety, low maintenance and long lifetime are essential requirements, high power density is also required, but energy density is not a limiting issue.
- Asymmetric SCs: This term is reserved for SCs that use two different *capacitor-like* materials to manufacture the electrodes and can achieve high energy and power densities [9], [14]. 30.4 Wh kg^{-1} and 5 kW kg^{-1} were reported for a MnO_2 Nanowire/ Graphene and Graphene asymmetric SC [41]. However, these SCs are still relatively expensive and may suffer from lower efficiencies and rated voltage due to the need for aqueous electrolytes [34], as well as from poor lifetime (79% of performance retention after 1000 cycles is reported in [41]). Therefore, asymmetric SCs could be suitable for applications in which the compromise between power and energy density is mandatory, and where cost is not a critical issue.
- Hybrid SCs: Composed of a capacitor-like electrode and a faradaic electrode, achieve a higher energy density, reported to reach values of more than 100 Wh kg^{-1} [42], [43]. By contrast, the power density is lower than the values achieved by symmetric SCs, around 4.5 kW kg^{-1} [40]. The development of this technology is less advanced than that of symmetric and asymmetric SCs. Even though there are already hybrid SCs available in the market [44]–[46], many papers have been published suggesting new materials and manufacturing processes [47], [48]. Recently, many hybrid systems have been reported, such as AC// PbO_2 [49], graphene//PbO_2 [50], AC//$Ni(OH)_2$ [51], AC//$Li_4Ti_5O_{12}$ [52] and AC//$LiMn_2O_4$ [53], [54]. Manufacturing methods dedicated to using original raw materials, such as egg white, were also suggested [55], obtaining a hybrid SC which shows promising power and energy density characteristics. Only values at material level are given in this paper (only the weight of the electrodes and electrolyte is taken into account). 257 Wh kg^{-1} and 867 W kg^{-1} (material level) with a performance retention of 79.2% after 15 000 cycles is reported in this paper.

D. TYPES OF SCS BASED ON THEIR ELECTROLYTE

- Organic electrolyte: An organic solvent, such as acetonitrile (ACN) or propylene carbonate (PC) is the basic component of these electrolytes. A salt such as Et_4NBF_4, whose organic ions are relatively large, is dissolved in the solvent. These ions should be able to access the electrode pores in order to contribute to the energy storage. Therefore, electrodes with micropores that are not able to host the ions are not suitable for organic electrolytes. Furthermore, the lack of micropores enhances the SC power performance. Their decomposition voltage can be as high as 2.2–3 V [56], contributing to the high power and energy density of the device.

  The most commonly-used organic solvents are PC and ACN, due to their low viscosity, high conductivity and electrochemical stability, making it possible to manufacture high-energy SCs that are able to deliver high power and high cyclic stability [57]. However, there are some safety concerns regarding the AN solvent, which is flammable and toxic [58]. Even though organic electrolytes are widely used, research efforts are currently focusing on the development of new, safe solvents to provide higher energy densities [59]. A solvent with a decomposition voltage of up to 4 V has already been presented [60]. However, the trade-off for this increase in the voltage window is a considerable reduction in the maximum power managed by the SC.
- Aqueous electrolyte: These electrolytes consist of small acid molecules, for instance, H_2SO_4, dissolved in water. Given the smallness of these inorganic ions, electrodes with micropores (diameter around 1 nm) such as T-carbons or carbide-derived carbons are preferred. The decomposition voltage limit of aqueous electrolytes is lower than that of organic electrolytes. Given that water dissociates in H_2 and O_2 at a voltage of 1.23 V, the stability of aqueous electrolytes is limited to a maximum voltage of 0.6–1.4 V [56].

  Research efforts in aqueous electrolytes are focusing on improving their electrochemical properties. The most noteworthy research trends in this respect are, on the one hand, the increase in their decomposition voltage,

which has already been reported to be up to 2.2 V [61] by the use of an aqueous electrolyte with high solvation energy. On the other hand, the cycle stability of aqueous electrolytes needs to be improved, and a promising approach is to use a protic ionic liquid as a solute for aqueous electrolytes [62].

- Room-temperature ionic liquids: These materials were initially considered as alternative solvents for aqueous electrolytes, thereby limiting their applicability. However, nowadays, they are known to be an alternative to solid electrolytes and are considered to be a promising electrolyte due to their operating voltage window, which is even wider than that of organic electrolytes, leading to a very high energy density [63]–[65]. Their components are also less toxic than organic electrolytes [66], while offering higher thermal stability [67], [68] and lower volatility [69], which increases the maximum operating temperature.

  The current high price of ionic liquids is not due to the material itself, but to the necessary purification cost. A better understanding of these materials as an SC electrolyte is expected to lead to less restrictive purity criteria and, therefore, to lower the price of ionic liquid SCs [63]. These materials are still at an early stage of development and, therefore, a significant research effort is being made to improve their properties. In this respect, two important research trends focusing on ionic liquids for SCs are, firstly, the design and characterization of additives to improve the performance of these devices [70], [71] and, secondly, the achievement of solvent-free (or solid-state) SCs, offering outstanding ionic transport properties [72], [73].

E. INTERACTION BETWEEN ELECTRODES AND ELECTROLYTE

The selection of the electrodes and electrolyte for a particular SC is not independent. There should be a match between the physical properties of both elements in order to maximize the SC capabilities. Regardless of the material or energy storage mechanism (covered above), SC electrodes are porous materials designed to maximize the usable interfacial area A. The larger the area, the greater the capacitance and, therefore, the greater the storable energy E. Moreover, given that these devices have no isolating material between the positive and negative charges (contained on the electrode and in the electrolyte), the separation distance between facing positive and negative charges, called Debye length d, is a molecular-order distance determined by the size of the electrolyte ions [74]. This small d, combined with the large surface area A, boosts the capacity achieved by SCs compared with conventional capacitors.

Therefore, the porous structure of the electrode material deserves special attention. Nanopore materials with smaller pores lead to higher surface densities. Currently, electrode materials with surface densities in the order of 1000 m^2g^{-1} can be manufactured [75]. However, in order to maximize the contact area between the electrodes and electrolyte, the nanopores should be large enough to host solved ions and to thereby actually contribute to the double layer capacitance. According to IUPAC recommendations [76], nanopores are classified according to diameter (Φ) in micropores ($\Phi < 2$ nm), mesopores (2 nm$< \Phi <$ 50 nm) and macropores ($\Phi >$50 nm). When manufacturing SCs, the most suitable size depends on the electrolyte. When the electrolyte comprises small acid molecules (e. g. H_2SO_4) and water as a solvent, micropores with a diameter close to 1 nm, such as T-carbons or carbide-derived carbons, are desirable. On the other hand, when an organic electrolyte is used, whose ions are considerably larger, then mesoporous electrodes are preferred, enabling faster ion access and thereby increasing the SC capacitance for higher charge and discharge currents. In fact, a number of experimental studies confirm the better performance of mesoporous electrodes with organic electrolytes while microporous electrodes are more suitable for acid electrolytes [75]. Therefore, the usable double-layer surface of an SC with an aqueous electrolyte is higher than that of an organic SC, with the associated capacitance improvement. However, the decomposition voltage of aqueous electrolytes is lower than that of organic materials. Organic materials are typically chosen as SC electrolytes taking into account the fact that, while the energy stored in an SC (E) is linearly related to C, it has a quadratic correlation with v [57].

Currently, intensive research is being conducted in materials science and engineering, focused on achieving the highest uniformity and accuracy in pore size. The authors of a recently-published study [77] propose a manufacturing method based on a nickel (hydro)oxide foam which, according to the reported results, achieves a good distribution in pore size. Other authors [78] propose the use of salt, so that the electrode material crystallizes around the salt ions, which are then removed using water. Surface areas as high as 1400–2100 m^2cm^{-3} have been recently reported for different electrode materials and manufacturing processes [79]–[81]. Moreover, significant research efforts are devoted to achieving electrodes for organic and ionic liquid electrolytes with higher surface areas. Graphene-based electrodes with an active area of up to 3100 $m^2\,g^{-1}$ have been published [82].

III. ELECTRICAL PERFORMANCE OF SUPERCAPACITORS

Following the analysis of the main electrode and electrolyte material properties performed in Section II, we will now go on to discuss the electrical implications, disclosing the reasons for the most noteworthy electrical phenomena and analyzing their impact on the SC performance, when it is part of an energy system. Greater attention should be paid to one aspect or another, depending on the particular requirements of each application, as covered in the following subsections.

A. VOLTAGE-DEPENDENT CAPACITANCE

Variable capacitance is one of the characteristic features of SCs. Although it is usually not critical to the SC performance,

since it does not represent a significant feature loss, it does need to be taken into account when the SC is part of an energy system. This is due to the fact that the capacity variation through the entire voltage range has been reported to be between 15% and 20% of the rated capacity [83], a figure that cannot be disregarded in most designs.

Capacitance is a magnitude that measures the amount of stored charge (q) for a given voltage difference (v):

$$C = \frac{q}{v} \tag{1}$$

This magnitude is of particular interest in traditional capacitors given that, as shown in (1), it is a characteristic property that relates charge stored in a device to its terminal voltage. However, the distance between charges in the double layer of an SC, d, lies on the atomic scale, and an increase in the voltage applied to this double layer intensifies the electric field in this zone, thereby increasing the force of attraction. This effect induces an increase in the density of stored charge, which means that the SC capacitance increases in line with the applied voltage. As a result, since C is a voltage-dependent parameter, (1) does not offer the same advantages as when working with conventional capacitors. This is the reason why differential capacitance C_{dif} is a preferred parameter when studying SCs. C_{dif} is defined as the ratio between the increase in the stored charge dq and the induced voltage variation dv:

$$C_{dif} = \frac{\mathrm{d}q}{\mathrm{d}v} = \frac{i\,\mathrm{d}t}{\mathrm{d}v} \tag{2}$$

Capacitance C and differential capacitance C_{dif} refer to the same property of an SC: the relationship between stored charge and voltage. Even though C is the parameter used to define conventional capacitors, C_{dif} is often chosen to describe SCs. The mathematical correlation between C and C_{dif} depends on the expression used to relate C to voltage v. If a linear dependency is assumed ($C = C_0 + kv$) — which is a typical approach in the literature [83]–[85] — then the correlation between C and C_{dif} can be deduced from the following expression of current i:

$$i = \frac{\mathrm{d}q}{\mathrm{d}t} = \frac{\mathrm{d}\,(Cv)}{\mathrm{d}t} \tag{3}$$

Substituting the linear expression for C_{dif}:

$$i = \frac{\mathrm{d}\,((C_0 + kv)\,v)}{\mathrm{d}t} = (C_0 + 2kv)\,\frac{\mathrm{d}v}{\mathrm{d}t} \tag{4}$$

and using the relationship shown in (2):

$$C_{dif} = C_0 + 2kv \tag{5}$$

Therefore,

$$C_{dif} = C + kv \tag{6}$$

In addition to voltage dependency, temperature is a factor that may affect the capacity of an SC. One of the main advantages of SCs is their good performance in extreme temperatures. However, the variation in the capacitance value produced by such large temperature fluctuations may require attention for the proper design of the energy system. Given the fact that a temperature increase causes a growth in the Brownian motion of the ions forming the double layer, there is a larger gap between the positive and negative charges in this double layer with increasing temperature, which leads to a decrease in capacitance [86]–[88]. In fact, a capacity loss of around 0.1% $^{\circ}\mathrm{C}^{-1}$ has been reported [83]. Assuming a temperature variation of 80 $^{\circ}$C, this means an 8% of divergence in C. Temperature usually has a lower impact than voltage on the value of C but may require attention for a system designed to operate outdoors.

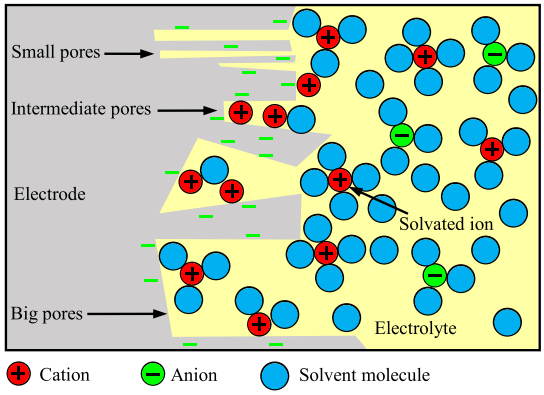

FIGURE 4. Desolvation of ions to access small electrode pores [83].

B. CHARGE DISTRIBUTION ALONG THE ELECTRODE SURFACE

The importance of a match between the size of the electrode pores and electrolyte ions has already been highlighted in subsection II-E. Nonetheless, it is important to point out that the solvents used in most electrolytes are polar (usually water as an inorganic liquid or an organic solvent such as acetonitrile). This polarity leads to molecular interactions with the solved ions and therefore ion solvation, which is an association process between solvent molecules and solute ions, as represented in Fig. 4 [34]. This process takes place in solvents with polar molecules since their partial charges are oriented towards ions, as a result of electrostatic attraction, thereby stabilizing the system. The importance of the match between pore size and ion diameter is also shown in Fig. 4. Pores with a Φ that is less than that of the electrolyte ions are too small to allow access and make no contribution to total capacitance. While those pores with a Φ that is greater than that of the solvated ions are totally accessible to the ions, and intermediate pores with a Φ between that of the solvated and non-solvated ions are available to the electrolyte ions that have undergone a desolvation process [89]. In this respect, in order to allow the ions to penetrate these intermediate pores, there is a need to break down the intermolecular forces established between the ions and the solvent molecules, a process which has its own dynamic behavior and requires energy.

Charge distribution processes have special relevance in applications requiring fast and deep charge–discharge cycles. In these situations, the SC provides its full power capability; however, the effect of these solvation dynamics is that it is not possible to fully charge or fully discharge at this high-current rate. The proportion of surface area that requires some degree of ion solvation and desolvation in a typical SC has been reported to be around 20% of the total electrode–electrolyte interface area [83].

C. OHMIC PHENOMENA

Electronic and ionic charge transport occurs during the SC charging and discharging process [87]. On the one hand, the Joule effect takes place in the electron conductors, whereby part of the electron kinetic energy is converted into heat due to friction with the conductor material. On the other hand, during the ionic charge transport process taking place in the electrolyte, part of the ion kinetic energy is converted into heat due to friction with the other atoms in the dilution. The voltage required to overcome both dissipative phenomena is proportional to the number of charges transported and, therefore, to current. This proportionality results in both these effects being grouped together and called ohmic phenomena.

Temperature variation has opposite effects on these two phenomena. For the solid electrode, an increase in the operating temperature implies the greater vibration of the atoms which, in most cases, results in an increased Joule effect with temperature. While, in the liquid electrolyte, it provokes an increase in the molecule mobility, resulting in a decrease in viscosity, implying a reduction in dissipated energy [90]. Some studies show that the weight of the ionic charge transport is considerably higher than that of the electric charges in the SCs [74], therefore, a temperature increase results in decreased ohmic phenomena.

Ohmic phenomena have a minor impact on SCs when compared to other electrochemical ESSs such as batteries. However, given the high power managed by SCs in typical applications, attention should be paid to this issue. On the one hand, ohmic phenomena provoke a voltage drop, which means a decline in SC energy efficiency. Since a significant advantage of SCs is their high efficiency [91], ohmic losses can take on a primary role in applications in which this parameter has the utmost importance. On the other hand, the dissipated heat needs to be evacuated in order to avoid danger due to overtemperature, which may require particular attention with regard to outdoor applications or SCs placed close to other heat sources.

D. ELECTRICAL SELF-DISCHARGE

Self-discharge is one of the main drawbacks preventing SCs from being used to store energy for times of more than 30 minutes [92]. In fact, the authors of [93] quantify the energy lost during the first two hours of storage as 36% of the useful energy stored in the SC. The main self-discharge mechanism in SCs is current leakage through the ion-conductive membrane separating both electrodes. The self-discharge effect is shown by a linear decrease in the SC voltage over time.

The SC self-discharge is one of the aspects that need to be improved and a number of research works have been published on this topic. In the same paper, some authors study self-discharge behavior, and ionic charge distribution in electrode pores [94]–[96]. Note that charge redistribution is measured as a nonlinear evolution of SC voltage over time during the first minutes or hours of voltage stabilization. However, this process does not provoke a discharge in the SC, since the electrical charge is still available in the SC even though the voltage is lower because more electrode surface area is used to build the double layer [97]. The authors of [93] rule out the self-discharge faradaic reactions as the reason for the nonlinear voltage change in SCs for two main reasons: (*i*) the v–ln t relationship does not have the characteristic linear trend of a faradaic reaction and (*ii*) the voltage at which this trend is measured is well below the decomposition voltage of the electrolyte.

Research works have also been published in which SC performance is enhanced by reducing self-discharge, proposing coatings for the electrodes which are able to reduce the leakage current [98], [99]. The drawback of this proposal is that the specific capacitance and energy storage density is also reduced by 56%. Other authors [100] assume this limitation imposed by self-discharge and propose management strategies in order to minimize the wasted energy.

E. HIGH-FREQUENCY BEHAVIOR

Supercapacitors are usually used for fast charge–discharge cycles, given their outstanding performance in these applications. Cycles lasting from tens of seconds to ten minutes are harmful to other ESSs, such as batteries, while SCs show their best performance within these timeframes. However, given that the charge and discharge processes involve the movement of ions through the electrolyte (mass transport), they are not able to manage frequencies as high as those managed by conventional capacitors. The usable capacitance (or equivalent capacitance) loss with increasing frequency has been studied in several papers [83], [101], reaching the conclusion that the equivalent capacitance of an SC has the behavior shown in Fig. 5. There is a cut-off frequency (which depends on the SC materials and manufacturing process, but it is usually around 1 Hz) where the device capacitance drastically decreases and no capacitive behavior is measured for higher frequencies. This is the reason why SCs cannot be used to filter the harmonic components of an electronic converter (several kHz). However, there are applications where intermediate frequencies need to be filtered, for instance, the harmonics produced by diode rectifiers (hundreds of Hertz). The use of SCs in these applications has also been studied [102], concluding that graphene electrodes are required in order to have a usable capacity at this frequency range. Therefore, the cut-off frequency shown in Fig. 5 for a graphene SC is in the order of hundreds of Hertz.

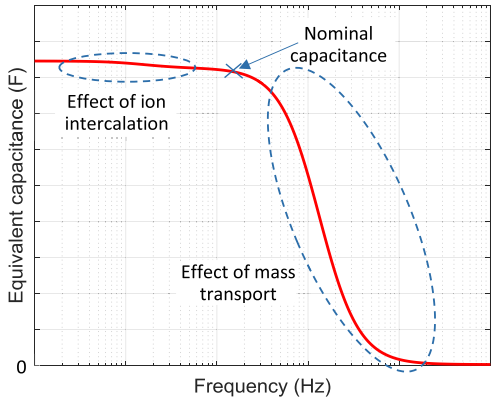

FIGURE 5. Equivalent capacitance as a function of frequency.

IV. MODELING AND PARAMETER CHARACTERIZATION

The model of a physical system is the mathematical representation of certain aspects of its behavior. Given the complexity of processes governing the behavior of any system and the considerable amount of variables having a greater or lesser influence on its performance, each model is designed with the aim of achieving particular objectives. The modeling of electrochemical systems, and SCs in particular, is an essential tool to exploit the electrochemical principles and optimize the integration and management of the SC in a complete electrical system. Moreover, this good interaction between material science and electrical engineering is useful for the improvement of SC materials and manufacturing processes, SC performance prediction, control strategy, lifetime prediction, cost calculations and future expectations.

A survey of the main modeling trends is presented in this section, identifying the major strengths and weaknesses of each one, and addressing the most reasonable functions of each model. The most-used characterization techniques for each model trend are summarized and the results of some experimental tests are presented as illustrative examples to facilitate the understanding of models and characterization processes. Given the system-integration focus of this review, more emphasis is placed on model trends focused on supporting SC engineering applications.

A. MODELING THE CORE PRINCIPLES OF DOUBLE LAYER BEHAVIOR

The double layer effect was initially described by the German physicist Hermann von Helmholtz [103]. He realized that a charged electrode submerged in an electrolyte repelled ions with its same charge and attracted the ions with the opposite charge [104]. He modeled this phenomenon as a conventional capacitor with distance for charge separation H, which is approximately the radius of solvated ions, as shown in Fig. 6 (a). The main weakness of this proposal is that capacity has no dependence on voltage, which is not in line with real measurements [105].

Subsequently, Guoy [106] and Chapman [107] independently developed a model for the double layer in which ion mobility is taken into account. Ions are threatened as point charges, and a combination of diffusion (statistical in nature) and electrostatic forces is proposed as the governing phenomena for ion mobility [104]. Therefore, a diffuse layer in the electrolyte region closest to the electrodes is proposed, as shown in Fig. 6 (b). However, since ions are considered as point charges, the capacity values predicted by Guoy and Chapman are larger than actual measurements because in reality ions have a finite size and they cannot approach arbitrarily close to the surface [105].

Stern [108] combined the Helmholtz and Guoy–Chapman models and described the double layer as a combination of the two layers shown in Fig. 6 (c). He proposed a compact layer of immobile ions strongly adsorbed to the electrode surface, similar to the Helmholtz layer, and a diffuse layer where ions have mobility and the Guoy–Chapman model is applied [104].

These are the original works in which the principles of the double layer behavior were established and the fundamental equations were proposed. Even though these ideas are used to develop SC models, they are not used by themselves to model physical devices, since the influence of other phenomena must also be taken into account in a model in order to predict the actual behavior of the SC.

B. MOLECULAR MODELS

Molecular modeling is a handy tool for the design of SCs and material properties analysis. Thanks to this technique, it is possible to predict phenomena that are not observable in any experimental set-up, such as the distribution and orientation of electrolyte ions, the change in the electrode morphology [58], influence of the ionic resistance of the separator on the SC performance, and the ionic and electronic resistance of the porous electrode [109].

Both the equilibrium state and dynamic phenomena which drive the SC behavior can be modeled through molecular modeling. With this aim, the behavior of the SC materials is studied at molecular level starting from the physicochemical laws governing the matter. Quite complex simulations need to be solved to run this kind of models, requiring the use of simulation techniques such as spectral element methods to discretize the model equations [110] or Monte Carlo, based on statistical mechanics or molecular dynamics, which solve Newton's equation of motion for a many-bodied molecular system over a short period of time [111], [112].

Both the accuracy and computational requirements of these models are mainly dependent on the modeling of electrodes and electrolyte. In this regard, a primitive model can be chosen, which considers ions as hard spheres and electrodes as simple walls, thereby reducing the simulation cost. However, the model accuracy is also reduced due to their unrealistic structural assumptions and its inability to calculate electrostatic properties. The other option for electrolyte modeling, which significantly increases the accuracy and computational cost of the model, is to consider the solvent molecules as uncharged hard spheres. The computational requirements of

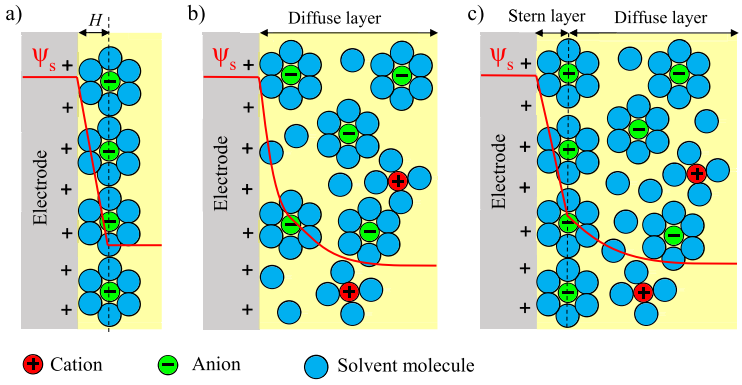

FIGURE 6. Schematics of the electric double layer structure showing the arrangement of solvated anions and cations close to the electrode–electrolyte interface in the Stern layer and the diffuse layer: Helmholtz model (a), Gouy-Chapman model (b) and Gouy-Chapman-Stern model (c) [104].

these all-atom electrolyte models limit their use, particularly in simulating large systems [113]. With the aim of overcoming these limitations, reduced-order [114], united-atom or coarse-grained models [58] are proposed in the literature.

There are also two main options for the electrode models. On the one hand, the voltage on each electrode atom at each molecular dynamics step can be assumed to be equal to a specified value [115], [116]. On the other hand, a simpler, computationally less expensive option is a simulation where fixed partial charges are assigned to each atom [117], [118]. As concluded in [119], the use of constant charge simulations alters both the structure of the adsorbed fluid at the interface and the time scales over which relaxation phenomena occur.

There are experimental techniques devoted to analyzing the material properties of an SC. The capability of these techniques for the characterization of working devices are of special interest in order to understand the performance of these ESS. In this sense, the nuclear magnetic resonance and electrochemical quartz crystal microbalance techniques are used in [120] to directly quantify the populations of anionic and cationic species within an SC electrode. However, the majority are specific techniques that do not allow for the testing of the SC as a whole, since access to the materials is required. The pore structure and its correlation with the size of electrolyte ions are of utmost importance in material characterization. A number of studies also analyses the reason for SC failures under different abuse conditions with the aim of preventing hazards, maintaining the integrity of other systems and protecting persons. These abusive conditions usually include high or low temperatures, high voltages and short circuits. After the SC death, it is disassembled and the state of its materials at this point provides valuable information for life extension and catastrophic failure prevention. Therefore, the experiments used to characterize standard materials are also used for post-mortem analysis [121].

These are the most salient approaches to the analysis of SC materials. The first material property that can be measured is the pore structure of the electrodes, whose diameters are in a nm or μm scale. The suitable size of these pores has a primary influence on the SC behavior, and several techniques are proposed to characterize this parameter. Scanning electron microscopy [122], volumetric gas adsorption or microwave measurement [79] are three of the most widely-used ones. A second property that is usually characterized is the lattice structure of these pores, which is several orders of magnitude smaller than the pore size (Å). The most-used experiments for lattice structure analysis are X-ray spectroscopy and nuclear magnetic resonance [121]. Finally, the third property that is usually of interest is the relationship between material properties and their electrical performance. This issue can be explored via electrochemical measurements for three-electrode systems with either a potentiostat or galvanostat [121].

C. TRANSMISSION LINE MODELS AND FRACTIONAL MODELS

A transmission line model, first introduced by de Levie [123], [124], is a tool to model the electrical impedance of an SC. It is a useful approach to switch from the local pore scale to the macroscopic scale of an electrode. Instead of taking into account all the trajectories that each of the adsorbed species follows, the transmission line is a suitable electric circuit representation of the overall behavior of an electrode. It consists of an infinite succession of electrode slices modeled as a resistance and a capacitance in order to simulate the progressive penetration of the charges into the electrode. Two transmission lines are represented in Fig. 7 to model both electrodes in an SC. These two transmission lines, as well as the bulk resistance of the electrolyte R_{bulk}, are put together in [125] to represent the behavior of a complete SC.

The number of branches included in a transmission line model is a decision that determines the accuracy of the model, the complexity of the parameter fitting procedure and the computational requirements. The higher the number of

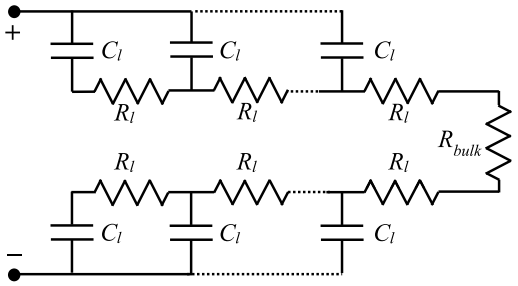

FIGURE 7. Equivalent circuit in the transmission line model. R_{bulk} is the resistance of the electrolyte in the bulk region, while R_l and C_l are the resistance and the capacitance inside the electrodes, respectively [125].

branches, the greater the number of time constants that can be taken into account and also the greater the computational requirements to perform the simulations. Depending on the application, more or less branches are preferable. Proposals for transmission lines with a variable number of branches, ranging from 5 [126] to 15 branches [127] can be found in the literature. Therefore, there are also authors that propose methods directed at reducing the simulation time in transmission line models, such as the authors of [126] who suggest a waveform relaxation strategy to reduce the simulation time while maintaining a good accuracy.

Parameter fitting is also a key topic in models of this type, given the high number of resistors and capacitors forming part of them. A parameterization method for a transmission line model based solely on equilibrium molecular dynamics is proposed in a paper [125] in which quantitative comparisons between molecular-scale simulations and electrochemical impedance experiments are advised.

Given that the transmission line model is based on the physical structure of the interface, it is useful to study the relationship between the physical properties of the electrodes and the electrical behavior of the SC. A transmission line model was combined with information on pore size distribution in [128] to simulate the frequency response of the entire electrode and to investigate the dependence of the relaxation time constant on several parameters. As a result, the authors determined a strategy to design the best mesoporous material for SCs with regard to energy and power density. The authors of [129] use a transmission line model combined with electrochemical impedance spectroscopy experiments and density functional theory to understand how redox reactions lead to the premature ageing of conducting polymers. In this way, they are able to propose new methods to increase the durability of these SCs and to improve their electrochemical properties.

Even though transmission-line models offer a number of advantages for the simulation of electrode impedance, one of their main drawbacks is that they are difficult to scale when several cells are connected in series or parallel [74]. Therefore, when a real SC system needs to be analyzed, analytical models, which are addressed in the following section, are usually preferred.

This dynamic behaviors of SCs is observed when a step current is applied to the SC, as shown in Fig. 8 (a). During the first 0.2 s following the current step, a variable slope is measured in the voltage response, which is different from the final slope represented in the figure by a green, dotted line. However, when the instantaneous response and the dynamic phenomena need to be separated, it is difficult to accurately determine the frontier between them, and the parameters calculated are not usually accurate enough. The experiments typically performed to characterize these phenomena are aimed at the quantification, discrimination and adequate representation of the variable behavior of an SC at different frequencies. The most interesting dynamics for an SC application in an energy system are related to the double layer response, which takes place for frequencies ranging from a few Hz to hundreds of Hz.

The most common experiment for this analysis is electrochemical impedance spectroscopy (EIS), consisting in the application of a small sinusoidal current perturbation with varying frequencies around a steady-state operating point and the measurement of the voltage response. A small perturbation is required since the behavior of the system is then linearized around the steady state. The complex impedance of the SC is determined using the generalized Ohm's law, and the result is represented in the Nyquist diagram, as shown in Fig. 8 (b). Note that the imaginary axis is usually inverted to have the capacity behavior plotted in the positive y-axis. From this graph, the impedance associated with the instantaneous phenomena can be calculated as the point at which the Nyquist plot intersects the real axis when there is neither capacitive nor inductive behavior. This instantaneous impedance obtained from the test shown in Fig. 8 (b) is 5.95 mΩ. A semicircle or semi-ellipse needs to be fitted to the central part of the Nyquist plot in order to calculate the influence of the dynamic phenomena associated with the double layer. Given the dynamic nature of the double layer, its impedance varies with frequency, as shown in the Nyquist plot.

From the impedance obtained with these experiments, the equivalent capacitance (C_{eq}) of the SC for various frequencies can also be calculated, as shown in Fig. 8 (c). As explained in subsection III-E, C_{eq} decreases at a frequency around 1 Hz, and there is also a frequency limit above which no capacitive behavior is measured. This frequency limit coincides with the point at which the Nyquist plot intersects the real axis in the EIS.

In addition to the aforementioned experiments, it is also possible to analyses larger fluctuations in the managed power. With this aim, sinusoidal currents with different amplitudes and frequencies are demanded from the SC. In the test shown in Fig. 9 (a), a sinusoidal current with an amplitude of 60 A and frequencies of 1 Hz, 10 Hz and 100 Hz is demanded from the SC, and the voltage response is measured. An illustrative representation of these results are the *i*–*v* curves shown in Fig. 9 (b). The *i*–*v* curve obtained with 1 Hz encloses a larger area and has a bigger slope than the other two curves. A larger

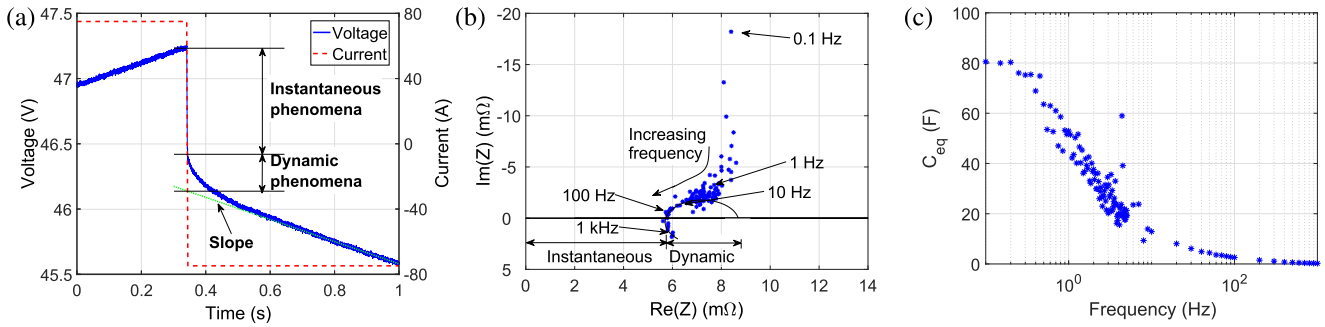

FIGURE 8. Dynamic performance of an SC measured in a Maxwell SC, model BMOD0083, with a rated capacitance of 83 F and rated voltage of 48 V: step experiment (a), electrochemical impedance spectroscopy (EIS) (b) and equivalent capacitance calculated from the EIS (c).

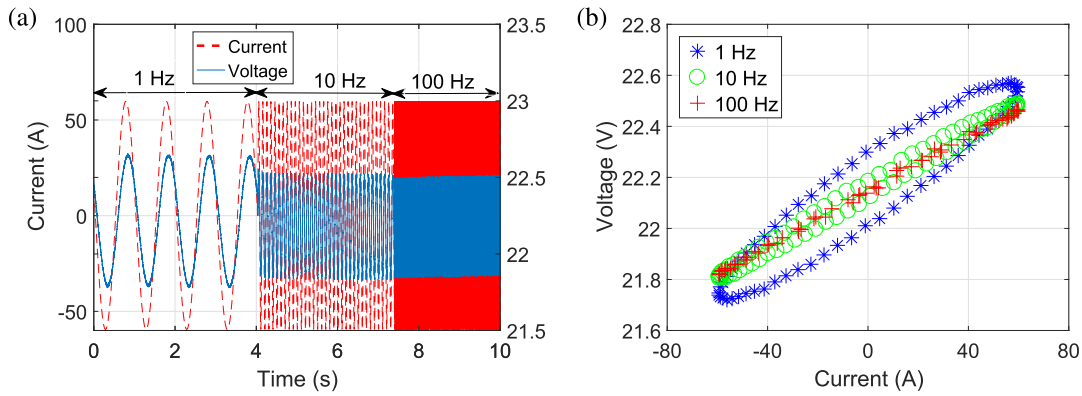

FIGURE 9. Sinusoidal experiment with high amplitude in a Maxwell BMOD0083: Current and voltage measurements for a 60 A experiment (a) and presentation of the results as *i–v* curves for easier analysis (b).

area is measured because there are dynamic phenomena with characteristic frequencies of around 1 Hz which provoke an offset between current and voltage, in accordance with the EIS shown in Fig. 8 (b). The bigger slope is due to the higher resistivity that the SC has at lower frequencies compared to that measured at high frequencies. The *i–v* curve measured at 10 Hz has a lower slope, due to the lower equivalent resistance at this frequency, and still enclosures a small area, since there are dynamic phenomena associated with the SC double layer, as shown in Fig. 8 (b). Finally, the 100 Hz curve has an even lower slope and no enclosed area, since no relevant dynamic effect has its characteristic frequency at this point.

An extension of transmission-line models that is commonly used in the literature are fractional models. Instead of representing he distribution of relaxation time constants as multiple RC branches, fractional models use elements such as Warburg impedances or constant phase elements (CPE). In fact, an infinite RC tree is equivalent to a single CPE. The behavior of these elements in the time domain is described by fractional-order differential equations, leading to fractional models.

D. SIMPLIFIED ANALYTICAL MODELS

Simplified analytical models are the next step after the transmission line models in the representation of the electrical performance of a complete supercapacitor. While transmission line models represent the impedance of an SC, simplified analytical models include other concepts such as coulombic efficiency, self-discharge and parasitic inductances. They are usually represented as equivalent electric circuits and are a suitable tool for the estimation of the electrical performance of SCs. This equivalent circuit representation is of particular interest for the analysis of installations in which the SC is one of the many systems involved, and an interaction of all these models is needed in order to simulate the entire plant.

The strategy followed to simplify and represent the physical phenomena as an equivalent circuit is an important topic to be addressed during the design of a simplified analytical model [130], [131]. The more the model is simplified, the lower its mathematical complexity and accuracy in the prediction of SC performance. The targeted accuracy and the frequency range of interest should be considered when selecting the most suitable model. The characterization of the SC behavior and the process to calculate the values of the equivalent circuit parameters is another important topic in which intensive research is being conducted [132], [133].

One of the main parameters involved in the SC modeling process is capacitance. Most of the simplified analytical models take into account the voltage dependence of SC capacitance. Some authors propose a tangential expression as shown

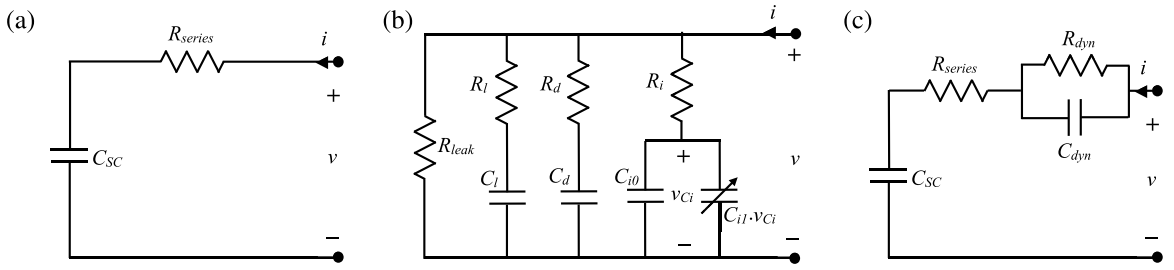

FIGURE 10. Basic electric circuit for SC modeling: simple RC circuit (a), multi-branch model (b) and dynamic model (c).

in the following equation [74]:

$$C = C_a + C_b \tanh\left(\frac{v}{U_x} - U_x\right) \tag{7}$$

where U_x is the voltage at the inflexion point of the hyperbolic tangent term, v is the supercapacitor voltage and C_a and C_b are fitting coefficients. Other authors use a linear expression to fit the voltage variability of capacitance [83]–[85]:

$$C = C_0 + kv \tag{8}$$

Besides this variable capacitance, simplified analytical models represent other phenomena that determine the supercapacitor electrical performance. The most commonly-used electric circuits used with this aim are:

- RC circuit: This model consists of an ideal capacitor and a series resistance which represents all non-ideal phenomena in the SC, as shown in Fig. 10 (a). Its main advantages are simplicity in the fitting process of its two parameters, fast computer simulation and good accuracy for fast dynamics [134]. It is generally used for the sizing of storage systems and the approximate calculation of system efficiency [135]. With the aim of significantly improving the accuracy of simple RC circuit models, some online fitting methods have been proposed in the literature [136].
- Multi-branch models: These model are built by the parallel connection of several RC branches with different time constants. These branches model the ion diffusion through the electrode pores. A suitable selection process for the time constant and the distribution of resistance and capacitance in these branches has been analyzed in the literature [137]. Three is the number of branches used by most authors [84]. A leakage resistance (R_{leak}) is also usually included to model the self-discharge of the SC, as shown in Fig. 10 (b). Some authors propose only two parallel branches, but they need to include a time-dependent leakage resistance [138]. Slow dynamics (tens of seconds or more) and self-discharge behavior are accurately predicted by these models. Several studies conclude that multiple-branch models achieve the best accuracy for the energy stored in an SC (state of charge) [139] and self-discharge [95].
- Dynamic models: These are built by the series connection of a capacitor representing the primary capacitance of the SC and some RC groups, as shown in Fig. 10 (c), thereby improving the accuracy of the model for high-frequency applications. They are particularly suitable for modeling fast charge–discharge cycles or rapid fluctuation in the supercapacitor power [140]. The conclusion of [4] is that the typical performance of the SC in an electric vehicle is best modeled by a dynamic model.

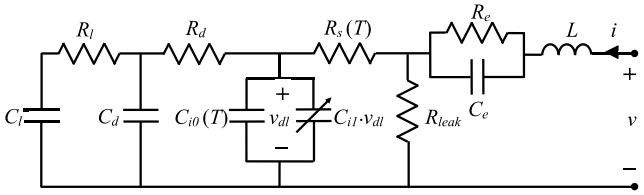

FIGURE 11. Equivalent circuit electric model proposed in [83].

Some research works propose multi-purpose models combining characteristics from the three types described above [83], [97], [141]. A model achieving accurate results in the prediction of the SC behavior for frequencies as high as 1 kHz and for the charge redistribution and self-discharge, which are only noticeable in a time span of several minutes, was presented [83]. One disadvantage of this model, shown in Fig. 11, is that it is slightly more complex than the types mentioned above. For this reason, the authors propose a test procedure aimed at circuit parameter calculation. Considerable effort was also made in this paper to correlate each of the circuit elements with the underlying physical phenomena which explain the behavior of the SC. Primary capacitance is represented in this model by the two capacitors situated in the central part of the schematic ($C_{i0} = C_{i00} + C_{i0T}T$ and $C_{i1}v_{dl}$). Capacitors C_d and C_l represent the capacitance of electrode pores smaller than the solvated ions. The energy required for the solvation and desolvation processes is related to resistors R_d and R_l, which are connected in series to each of the capacitors. Moreover, resistor R_s represents the ohmic phenomena taking place in the SC. Resistor R_{leak} is the leakage resistor and represents the electrical conductivity of the membrane, i. e. the SC self-discharge. The parallel connection of R_e and C_e represents the dynamic behavior of the porous electrodes. R_e is related to their resistance to electron movement and C_e is the parasitic capacitance, a consequence of their porous structure. Finally, L represents the inductance due mainly to

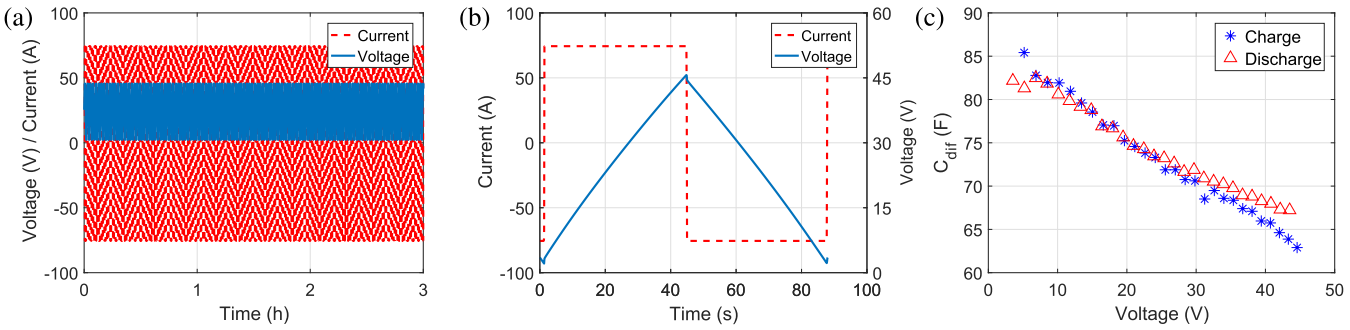

FIGURE 12. Current and voltage experimental measurements of the full-cycle test in a Maxwell BMOD0083: Overview of the whole test (a) and zoom view of one of the last cycles (b). Differential capacitance calculated with the measured data (c).

the electrical connections between the cells making up the module.

Given the applicability of these models, the experiments devoted to parameter calculation are of particular interest to engineering applications. The experiments depicted in subsection IV-C concerning transmission line models are also useful for simplified analytical circuits. However, other phenomena such as the simple measurement of SC capacitance, coulombic and energy efficiency, charge distribution in the electrode pores and self-discharge need to be addressed for some of the simplified analytical models. A set of two experiments which are typically used in the literature is proposed herein for the characterization of these parameters.

The first test consists of a series of full charge–discharge cycles with a constant current demand, as shown in Fig. 12. The experiment needs to be long enough for the SC dynamics to stabilize. As shown in Fig. 12 (a), the test lasted 3 hours. The current demand has a stepped profile with values of +75 A or –75 A, which entail a quasi-triangular shape in the voltage ranging from 3 to 45 V, given that the maximum voltage range is 0 V–48 V. The analysis is made in one of the last charge–discharge cycles in order to achieve a steady-state performance, such as the one shown in Fig. 12 (b). It is interesting to note in this figure that the slope of the voltage decreases when the voltage is higher. From this slope ($\mathrm{d}v/\mathrm{d}t$) and the measured current (i), the differential capacitance can be calculated using (2). This variable capacitance is shown in Fig. 12 (c). As explained in subsection III-A, a lower slope implies lower capacitance values. Coulombic and energy efficiencies can also be calculated as shown below:

$$\eta_c = \frac{\int_{t_m}^{t_{end}} i\,\mathrm{d}t}{\int_{t_0}^{t_m} i\,\mathrm{d}t} \tag{9}$$

$$\eta_e = \frac{\int_{t_m}^{t_{end}} i\,v\,\mathrm{d}t}{\int_{t_0}^{t_m} i\,v\,\mathrm{d}t} \tag{10}$$

where t_0 represents the time at the beginning of the cycle, t_m the time where the sign of the current is changed and t_{end} the time at the end of the cycle. The results obtained in the presented test are $\eta_c = 0.9985$ and $\eta_e = 0.9285$.

The other experiment for this characterization is the charging of the SC to a voltage close to the permitted maximum and the relaxation of the open circuit voltage over several days, as shown in Fig. 13. The current and voltage during the whole test are shown in Fig. 13 (a), and the charge distribution in the electrodes is illustrated during the first minutes or hours of measurement, as zoomed in Fig. 13 (b). The linear decreasing voltage recorded after the first hours of the experiment is due to SC self-discharge. The value of the leakage resistor (R_{leak}) can be calculated considering an ideal capacitor being discharged through the resistor. The following equation can be applied:

$$R_{leak} = \frac{v}{C_{dif}\,\mathrm{d}v/\mathrm{d}t} \tag{11}$$

The value obtained from this experiment is $R_{leak} = 193.9\,\mathrm{k}\Omega$.

Ageing phenomena also have particular relevance for SC simplified analytical models and their engineering applications. When the effect of ageing in SCs needs to be studied, the characterization of its electrical performance with the above-described tests is combined with methods directed at accelerating the ageing process in order to conclude the experimental work within a reasonable time frame. The temperature and operating voltage are usually increased, since the ageing rate doubles if either the cell voltage is increased by 100 mV, or the temperature is increased by 10 K [142]. It is noteworthy that a performance recovery phenomenon associated with cycle interruptions has recently been reported in a paper in which an empirical model for the state-of-health prediction is proposed [143]. Moreover, the influence of high-frequency ripple currents in SC ageing has been experimentally studied [144], concluding that they have no effect on SC ageing. Torregrossa and Paolone studied SC ageing phenomena in closer detail in a two-part article. Experimental measurements of capacitance decline and resistance increase under high-pulsed current and high temperature are presented in Part I [145]. They conclude in this paper that, while the SC capacitance decline is enhanced with a pulsed current, this stress condition does not affect resistance increase. The measurements performed in the previous paper allow the authors to present an ageing model in Part II [146] whose good performance is experimentally validated.

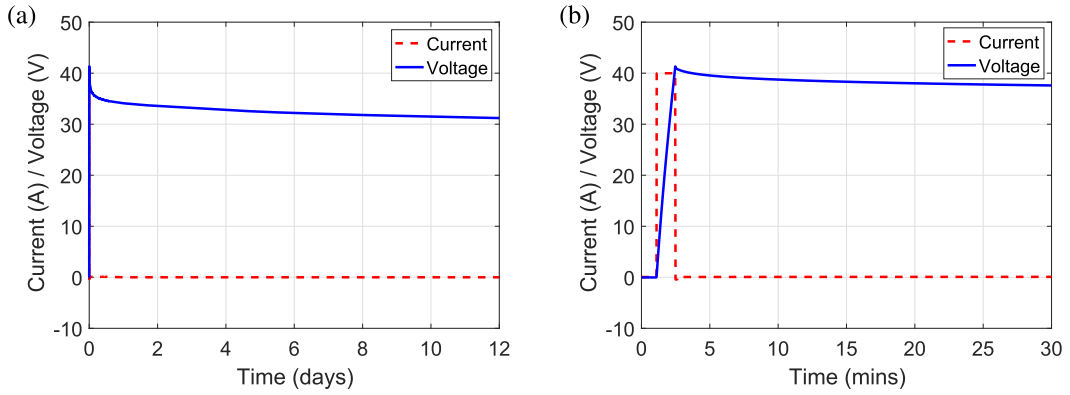

FIGURE 13. Stabilization experiment of a Maxwell BMOD0083: entire voltage and current measurements during 12 days (a) and zoom view of the first 30 minutes (b).

E. THERMAL MODELS

The thermal modeling of SCs is a useful tool to calculate working temperature T. The inputs for these models are usually the electrical performance of the SC (v and i) and the ambient temperature T_a. The knowledge of the SC internal temperature is necessary, given that it has several effects on the electrical properties of the device. Specifically, an increase in T provokes a decreasing series resistance of the SC and increasing capacitance [90], [147]–[149]. Moreover, high values of T accelerate the self-discharge of the device and parasitic chemical reactions, such as oxidation, following Arrhenius law, which means a faster ageing of the SC [150]. A thermal model consists in:

- Heat generation: Two kinds of processes generate heat during normal SC operation. On the one hand, there are ohmic losses due to the internal resistance which induce an overall increase in temperature. On the other hand, a reversible heat generation (or entropic term) is usually included in thermal models to model the entropy change in the double layer and to achieve better accuracy [140]. The most suitable model for this entropic term is still an open discussion in the literature. Most authors base their entropic heat generation on the approximate model proposed in [151], in which a single-atom double layer is assumed. However, in a recent comparative paper [152], the authors conclude that better results are obtained if the Poisson-Nernst-Planck equation is combined with heat equation, as suggested in [153].
- Heat transmission: Besides heat generation, the SC temperature T depends on the ability of the device to transfer this heat to the surrounding air. There are three heat transmission mechanisms, namely conduction, convection and radiation. Heat is transferred inside the solid from high to low temperature zones based on conduction phenomena. Convection (either natural or forced) allows the heat to be transferred from the surface of the device to the surrounding air. A thermal model whose equations are the fundamental heat transfer laws is proposed in [154] and has been used in the following research works like [155]. Given the small temperature difference between the SC surface and the ambient air, many authors disregard the effect of radiation as a heat transfer mechanism [83], [156], [157]. Enclosed modules comprising several cells and cooled by natural convection are usually modeled as thermal equivalent circuits, like the one proposed in [83] and shown in Fig. 14. The generated heating power $\dot{Q}_{gen}$ is dissipated through the module, the module thermal capacity is represented by C_{th} and the conduction and convection mechanisms are grouped and quantified by thermal resistance R_{th}. For the cases in which an airflow is forced around the cells to improve the heat dissipation, some authors propose modeling the process with an equivalent thermal circuit [156] while others prefer Fluid Dynamic Software to increase the accuracy of the model [157].

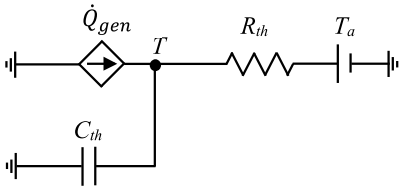

FIGURE 14. Thermal model for an SC module proposed in [83].

A usual approach to experimentally characterize the thermal performance of an SC is by achieving an almost constant heat power generation in the device resulting from its normal operation. The accuracy of the results is increased if the thermal characterization is performed with a constant ambient temperature, which can be achieved by placing the SC inside a climate chamber. The interior and ambient temperatures need to be measured since the difference between these two variables is related to the heat dissipation phenomena. With this aim, the experiment shown in Fig. 15, is conducted, consisting of charge–discharge cycles with a constant, stepped current until the SC temperature stabilizes, followed by a cooling period until the SC reaches ambient temperature. The heat generated during the first period can be assumed to be constant, and the temperature evolves as a first-order process.

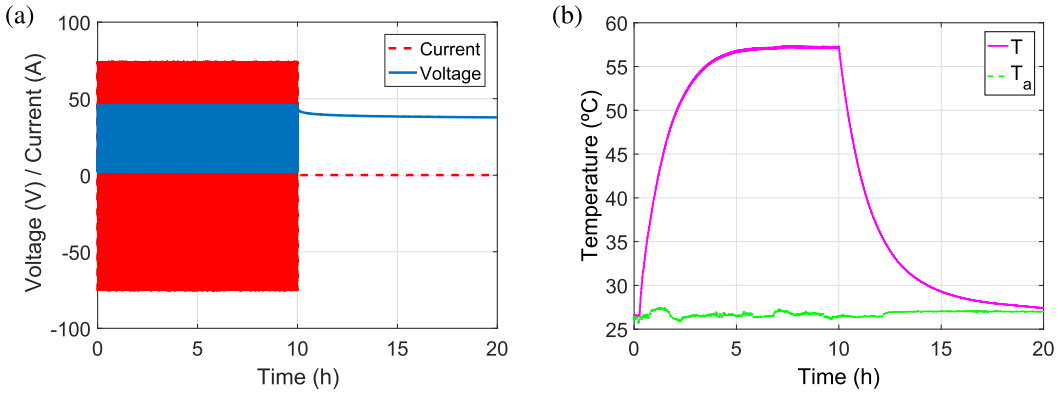

FIGURE 15. Thermal characterization of a supercapacitor Maxwell BMOD0083: current and voltage during the experiment (a) and interior (T) and ambient (T_a) temperatures (b).

The stabilization of T is required to adequately characterize this phenomenon, as shown in Fig. 15 (b). After this stabilization, when the current demand stops, the SC cools down to ambient temperature. The calorific power generated and the dynamics of the heat exchange process can be determined by this experiment.

V. SUPERCAPACITOR APPLICATIONS IN ENERGY SYSTEMS

SCs are experiencing rapid market growth and catalogue diversification thanks to their high power density, fast electrical response, long maintenance-free lifetime and their ability to perform in a wider temperature range than other ESSs. This section starts with a summary of some issues about the SC manufacturing process, it then goes on to present a survey of the main characteristics of the products available in the market and, finally, a critical analysis of successful and recently-emerged SC applications is made, classifying them into the four top market sectors.

A. SUPERCAPACITOR MANUFACTURING BASICS

As explained in Section II, the main components of an SC are the electrodes and the electrolyte. However, they also have a separator, to prevent short circuits inside the SC and metal current collectors attached to each electrode to drive the current from the electrodes to the external circuit and vice versa. The thickness of each electrode layer deposited on the current collectors and the deposition technique are of central importance in achieving good electrochemical properties and a long device lifetime [122].

Most commercial supercapacitor cells are cylindrical, such as the product shown in Fig. 16 (b). This shape is achieved by rolling up a jelly roll consisting of two aluminum foil current collectors with the electrode active material deposited on both sides. The porous paper separator is located between both electrodes to prevent short circuits, as shown in Fig. 16 (a). As can be seen in the figure, the positive and negative output terminals are on the top and bottom of the jelly roll. Once rolled-up, the jelly roll is impregnated with the electrolyte

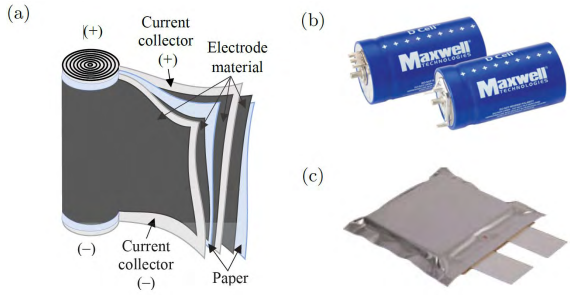

FIGURE 16. Jelly roll schematic (a) and two commercial SCs: Maxwell cylindrical SC (b) and Ioxus pouch SC (c).

and enclosed into a hard case to prevent the evaporation of the electrolyte and the contamination of the active materials. Following the trend addressed by the world's leading manufacturer, Maxwell Technologies, the cell diameter has been standardized to 60 mm. The height of the can has the required size to achieve the desired capacitance.

Given the easy automation of this manufacturing technique, cylindrical SCs are cheaper to manufacture and, therefore, used in most applications. The main drawback of this circular shape is that the heat generated inside the cell must be conducted through a thick material layer in order to be evacuated. Even though SCs have a high efficiency and the power losses are proportionally low, temperature can be a limiting factor on the maximum manageable power.

Pouch supercapacitors, such as the Ioxus device shown in Fig. 16 (c) have been designed to improve thermal conductivity. In this case, the manufacturing process consists of cutting and stacking current collectors, electrodes and separators. Electrodes with the same polarity are connected in parallel, and the whole device is sealed in a plastic bag. These devices are usually more expensive than cylindrical ones but are suitable for higher power densities.

Intensive research to reduce the price of SCs is currently being conducted. On the one hand, low-cost materials are being designed. A recent research work reports on a new electrode material which achieves a 90% price reduction by

TABLE 3. Characteristics of the supercapacitors offered by the main manufacturers.

Company	Country	Type	Device	C (F)	V_R (V)	ρ_e (Wh kg^{-1})	ρ_p (kW kg^{-1})	T_{op} (^{o}C)	Applications
Maxwell [46]	U.S.A.	Sym.	Cell	1–3400	2.3–2.85	0.7–7.4	2.4–14	–40/65	Transport,
			Module	5.8–500	16–160	2.3–4	3.6–6.8	–40/65	energy
LS Mtron [166]	Rep. Korea	Sym.	Cell	100–3400	2.7–3	3.3–7.5	0.9–2.4	–40/65	Industry, electronics,
			Module	2.5–500	16–381	2.3–5	0.3–0.6	–40/65	transport
Nesscap Co., Ltd [167]	Canada	Asym.	Cell	50–300	2.3	4.8–8.8	4.9–6.2	–25/60	Heavy vehicles,
		Sym.	Cell	3–5000	2.3–2.7	2–5.7	6–17	–40/85	pitch control,
			Module	1.5–500	5–125	1–3.7	2.5–6.8	–40/85	solar tile
Panasonic Corp [168]	Japan	Sym.	Cell	3.3–100	2.3–2.7	1.4–4.1	0.29–3.65	–40/70	Electronic
			Coin	0.1–1.5	3.6–5.5	0.13–1.5	10^{-3}	–40/85	devices
Vinatech [44]	Rep. Korea	Hybrid Sym.	Cell	10–800	2.3	4–12	0.4–0.8	–25/60	Transport,
			Cell	1–3000	2.5–3	0.7–6.5	1–11.3	–40/70	UPS, wind
			Module	2.5–60	16–144	1.7–5.6	0.4–4	–40/70	turbines
Yunasko [45]	Ukraine	Hybrid Sym.	Cell	1.3 Ah	2.7	37	4	–40/60	Transport,
			Cell	400–3000	2.7	4.7–6.2	7.1–41	–40/60	industry,
			Module	13–500	16–90	3.9–2.1	3.3–11.3	–40/60	electronics
Ioxus Inc [169]	U.S.A.	Sym.	Cell	1250–3150	2.7	4.5–6.3	23–34	–40/85	Transport, renewable
			Module	21–500	16–162	2.2–3.8	0.2–0.4	–40/85	energy, backup
SPS Cap [170]	China	Sym.	Cell	1–5000	2.5–2.7	0.9–6.5	0.5–8	–40/60	Transport, wind
			Module	0.5–500	16–2300	1.4–3.6	0.3–0.7	–40/60	turbines, micro grids

decrementing the SC capabilities by 50% [163]. On the other hand, manufacturing processes and materials for flexible SCs are being investigated. These soft ESSs are expected to be a key component of next-generation electronics. Given that flexible SCs are still not commonly available in the market, their manufacturing technique is to be developed during the upcoming years. A number of review papers [164], progress reports [165] and research papers [166]–[168] have been published recently establishing the basics of this new market sector. In this line, printed SCs are also a technology under research [169].

B. SUPERCAPACITOR MANUFACTURERS AND PRODUCTS

The purpose of this subsection is to present a comparative analysis of the products offered by the main SC manufacturers. Therefore, eight representative manufacturers have been selected, as shown in Table 3. Maxwell Technologies, which leads the SC global market, is represented in the first row of the table. The key features of each product are stated in columns 5–9, which are capacitance (C), rated voltage (V_R), energy density (ρ_e), power density (ρ_p) and operating temperature (T_{op}).

As covered in Table 2, symmetric SCs (Sym. type in Table 3) are the most common option and are offered by all the manufacturers. Of the companies summarized herein, only Vinatech and Yunasko offer hybrid models, while Nesscap has asymmetric SCs (Asym. type in the table) in addition to their symmetric options. As part of their symmetric SC products, most of the companies complement their offer of cells with standard modules, built by a number of series connected cells, whose characteristics are also summarized in Table 3. Besides these standard modules, most companies offer the option of customized modules adapted to the power and energy requirements of each customer, which are manufactured by the series or parallel connection of the required number of cells. These modules can be connected in series or parallel to meet the energy and power requirements of any particular application. Panasonic is the only company which centers its whole product line on SC cells and coin SCs, which are the series connection of two cells.

The parameters covered in the table are useful decision tools for the selection of the most suitable SC for each application. Firstly, there is a high range of capacitance values since greater or lower capacitance is achieved by using a bigger or smaller electrode in each cell. Conversely, the cell voltage depends on the SC technology instead of on the size and, as explained in Section II, its enhancement is a current research topic directed at achieving increased SC energy content. Although the rated voltage range offered by all manufacturers is tight (2.3–3 V), this difference has sensitive implications, given that the company that is able to provide the cell with the highest rated voltage (3 V) also has the highest energy density for a symmetric cell: 7.5 Wh kg^{-1}. The voltage range offered for the standardized modules varies considerably and is not as interesting as the cell voltage, given that modules are built by the series connection of many cells. Limiting factors for the series connection of SC cells are the requirements of voltage equalization and the electrical isolation of the metal components, which are easier to overcome than the material properties determining the cell voltage.

The comparison between SC energy and power density is also interesting. As shown in the Ragone Plot (Fig. 1), these devices can provide high power (several kW per kg), while the stored energy is not exceptionally high (a few Wh per kg). It is significant that the power and energy densities for modules are lower than those reported for individual cells, given that, apart from the actual cells, the manufacturing of a module requires, connections, safety devices and the module shield, making the module heavier than the sum of the weight of single cells. In a comparison of energy and power densities between different SC technologies (symmetric, asymmetric and hybrid devices), the data provided in Table 2 are

(a) (b)

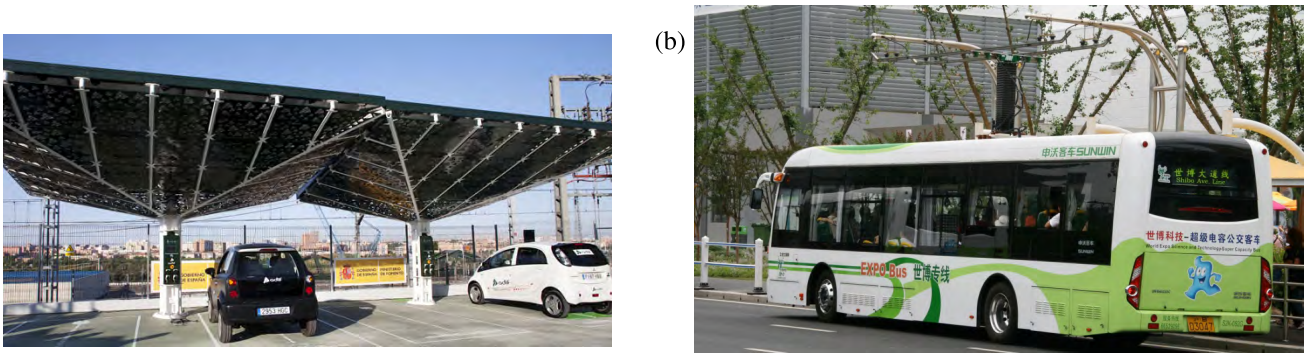

FIGURE 17. Transport applications of SCs: Electric car charging station in the foreground and railway track in the background. Lithium batteries and supercapacitors are used for the regenerative braking of railways and fast charging of electric vehicles [170]. Reproduced by kind permission of Adif (a) and Capabus charging its ESS based on supercapacitors. Reproduced from Wikipedia (b).

supported herein. Regarding energy density, symmetric cells achieve a maximum of 7.5 Wh kg^{-1}, while asymmetric cells reach 8.8 Wh kg^{-1} and hybrid cells 37 Wh kg^{-1}. Conversely, power density presents the opposite trend, given that hybrid cells achieve only 4 kW kg^{-1}, asymmetric cells 6.2 kW kg^{-1} and symmetric cells up to 41 kW kg^{-1}.

The wide temperature range in which any of the cells can operate is one of the key features that make SCs an advantageous option compared to batteries. While lithium-ion batteries cannot perform below 0 ^{o}C and the minimum temperature for lead–acid batteries is –20 ^{o}C, SCs can safely and reversibly operate at –60 ^{o}C. Asymmetric and one of the two hybrid cells covered in Table 3 have the narrowest operating temperature range (–25 to 60 ^{o}C), which is still wider than the safe window of most batteries. The last column of the table summarizes the applications suggested by each company for their products, providing a tentative approach to the selection of an SC. However, given the wide range of products offered by each manufacturer and the distinct requirements of each particular energy system, engineering applications of SCs are analyzed in detail in the following subsection.

C. ENGINEERING APPLICATIONS

1) TRANSPORT SECTOR

Supercapacitors provide substantial benefits to railway electricity systems. This technology has been used for many years to allow the regenerative braking of trains and to stabilize the catenary voltage. Two early examples are cities such as Cologne and Madrid, where trackside storage systems called SITRAS SES, built by Siemens using Maxwell's 1344 supercapacitors [171], have been installed since 2001 and 2003 respectively. Another example of such an application is located in south-eastern Pennsylvania, where trains stop and accelerate several thousand times per day. These stop-and-go processes have a duration of between 15 to 20 seconds. The transport authority installed a hybrid SC-battery ESS which captures excess braking energy from the trains by detecting a rise in the line voltage on an overhead catenary system. As a result, a reduction of 10–20% in electricity consumption was achieved, as well as 800 kW of fast response load modulation support to the grid operator, which is a paid service that can provide more than $200,000 in annual revenues [172].

Railways systems are also addressed in research and development projects. For instance, *Ferrolinera*® projects were carried out in Spain by ADIF, the public entity that manages the railway infrastructure. In this project, a hybrid lithium battery–SC ESS is used not only to enhance the regenerative braking of trains and grid quality but also to allow for the fast charging of electric vehicles through a fast charger connected to the railway electricity grid, as shown in Fig. 17 (a). Scientific papers proposing future SC applications to improve the transport sector have also been published. In this line, a management strategy to improve the energy efficiency in light railway vehicles through SC-based ESS is proposed in [173]. Some scientific papers propose installing SCs in trams [174] or trains [175], where the authors propose a SCs as ESS for a catenary free tramway equipped with an inductive power transfer system. However, trackside systems are more common in commercial applications due to the smaller size of the overall ESS and the lower installation cost.

Another important niche markets for SCs are urban buses. Due to their frequent stop-and-go driving conditions, SCs provide attractive characteristics for this application. There are proposals concerning hybrid battery–SC ESSs for electric buses [176], as well as commercial urban electric buses which rely only on SCs to store the required energy to reach the next stop. Buses of this kind, also known as *Capabuses*, are fitted with two roof-mounted pantographs for flash-charging the SC-based ESS at bus stops, as shown in Fig. 17 (b), and SCs provide the energy needed during the driving time between two stops. New ideas about the best strategy to size and manage SCs in city buses are being investigated. In this line, Song et al. published a research work in which the influence of the driving cycle of city buses on ESS design and control is studied using fuzzy pattern recognition [177].

Apart from railway systems and buses, the use of SCs in passenger cars is also increasing [178], in fuel, hybrid and

electric vehicles alike. An example of SCs in a commercial fuel vehicle is the Mazda i-ELOOP, which has a combustion engine and supercapacitor-type regenerative braking, achieving fuel savings of 10% according to the manufacturer's website [179]. Moreover, supercapacitor companies such as Ioxus offer an SC product line directed at either supporting or replacing traditional batteries for combustion engine starting [161]. Regarding hybrid vehicles, supercapacitors are used in micro-hybrid (or stop-go hybrid) vehicles such as Peugeot e-HDI as well as in full hybrid vehicles such as the Toyota safety braking system [180]. Research papers have also been published proposing the use of SCs in hybrid heavy-duty vehicles to achieve fuel savings [181]. In full electric vehicles, SCs provide faster acceleration, extended battery life and increased range. They exhibit the capability of absorbing regenerative braking energy, thereby limiting the high charging current to the battery. Therefore, a number of studies propose management strategies [182], [183] for dual SC–battery ESSs for electric vehicles. Specifically, two meta-heuristic methods are theoretically and experimentally compared in [182], while an SC is added to the Tazzari Zero battery ESS in [183] in order to lower the stress of the battery, thereby extending its lifetime. As an alternative to batteries, fuel cell–supercapacitor hybridization is also a current research topic concerning the most suitable management and control strategies for such a system, given the fuel saving, increased efficiency and enlarged FC lifetime provided by the SC [184], [185].

Additionally, the aerospace industry is focusing its development efforts on achieving a more-electric aircraft. An increasing number of electric devices are proposed, such as emergency power systems for aircraft. The high power peaks that are required from these ESS and the requirements for a long lifetime make SCs an attractive option to be installed along with batteries or FCs to create a hybrid ESS [186]. The management strategies of such a hybrid ESS is a key issue with regard to weight and volume minimization, as well as cost reduction [187].

2) ENERGY SECTOR

The energy sector is characterized by stationary applications in which SCs are chosen because of their outstanding power characteristics. Moreover, the extreme conditions that SCs are able to withstand and their low maintenance requirements make these systems especially attractive for renewable energy-related applications [189]. This sector has shorter time-to-market periods than transport applications, with time requirements of between one to three years [45].

One of the primary uses of SCs in renewable energy systems is the pitch control of wind turbines. According to the leading manufacturer Maxwell Technologies Inc. [190], 20 to 30% of wind turbines are equipped with SC pitch control systems, while 35 to 45% include a battery ESS instead. With regard to the conditioning of the actual wind power generated, many researchers propose SCs as a solution to deal with high-dynamic issues (faster than 1 minute). Power curtailment is a major concern associated with the increasing wind generation. Wind power intermittency has been detected as a remarkable cause of this curtailment, and SCs have been proposed to reduce this issue [191]. Some authors propose the sole use of SCs to deal with wind intermittency both with full converter [192] and double-fed induction turbines [193]. The hybridization of SCs with flow batteries has also been studied by means of simulation [194]. This hybrid system smooths the power output, lowering the battery cost and enhancing its lifetime and overall efficiency due to the inclusion of SCs. Attention should be paid in this kind of hybrid ESSs to the control strategy [195] and to its balancing [196], given the additional power flow that needs to be controlled after the inclusion of an additional ESS. Besides wind energy, SCs are proposed to be installed in other types of renewable generation plants for fluctuation suppression [197], low voltage ride through, voltage control support [198] and oscillation damping. Remarkable growth is expected for this sector, given that more restrictions are expected to be imposed on renewable energy generation [199]. For the same purpose of dealing with high dynamics, SCs can be used as a solution for solar firming. This is evidenced at a plant located in California, where the increasing intermittent solar and wind energy installations threatened grid stability. Since only 20 to 30 seconds of energy storage were required, an SC storage system was designed to demonstrate the capability of smoothing short term solar power fluctuations and providing ramp rate control [172]. A step forward from this firming application, there are also studies proposing SCs to be used for grid regulation services [200], [201].

Electrical microgrids are usually equipped with renewable energy generators while the grid connection, when available, is often controlled to minimize the disturbance caused by the microgrid. Therefore, the selection of the most suitable ESS and its management strategy are of primary importance [202]–[204]. SCs have useful characteristics that can improve the microgrid ESS. For this reason, SCs are used in stand-alone microgrids to improve the resiliency [205], or to deal with fast load fluctuations [206], [207]. They are also useful in grid-connected microgrids [208], [209]. As an illustrative example, the role played by SCs in an experimental microgrid installed at the Public University of Navarre is herein analyzed [210]. The energy requirements of this microgrid are covered by a hydrogen-based system with a capacity of 40 kWh. An SC bank is included with the aim of managing power fluctuations caused by renewable generation and consumption. Given that power demands with a frequency of a few hertz shorten the lifetime of fuel cells (FCs) and electrolyzers [211]–[213], in line with these results, some authors propose, for the above-mentioned microgrid, an SC bank that is able to manage frequencies of more than 3 mHz. These requirements were met with three Maxwell BMOD0083 SC modules that offer 82 Wh of storage. The SCs and FCs are directly connected in parallel, as shown in Fig. 18 (a). This hybrid ESS makes it possible

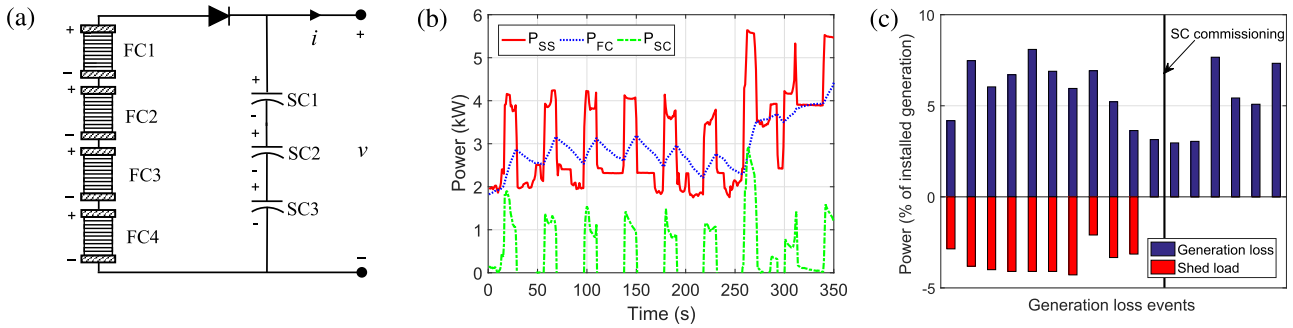

FIGURE 18. Effect of SCs on electricity systems. Electrical connection of the ESS of a microgrid (a), power measurements on the 12th of December, 2012 at 20:00 h in the mentioned microgrid: Power required from the ESS (P_{SS}), which is shared between the SC subsystem (PSC) and the FCs (P_{FC}) (b) and performance improvement of the electricity grid of La Palma island due to a 4 MW, 5.5 kWh SC module installed by Endesa [188] (c).

to achieve a higher overall efficiency and a longer lifetime of the hydrogen subsystem.

Fig. 18 (b) shows the power of the FCs and SCs during 350 s of microgrid performance. The power of the ESS (P_{SS}) is the sum of the fuel cells power (P_{FC}) and the supercapacitor power (P_{SC}). The fast frequencies are managed by the SCs, allowing a better performance of the FCs. The fastest variation of P_{SC} takes place between $t = 257$ s and $t = 262$ s, when P_{SC} increases from 0 to 2.93 kW in only 5 s. Conversely, the fastest growth in P_{FC} takes place at the same time but has a much lower gradient, from 2.31 kW to 3.5 kW in 15 s.

There are also weak grids whose stability is threatened by voltage fluctuations. Such networks can be found, for instance, in small islands, such as La Palma (Canary archipelago, Spain). The DSO Endesa is using SCs for a double purpose on this island. Firstly, they provide a fast response which improves the spinning reserve of diesel units. Secondly, the SC system prevents load shedding, which is a protocol that disconnects electricity users from the grid in the event of frequency deviations. Specifically, an LS-Mtron SC system with a maximum power of 4 MW and an energy content of 5.5 kWh was installed in 2013. The outstanding power capacity of SCs is exploited in this project since they are completely discharged in just 5 seconds. This experience has reported good results, as shown in Fig. 18 (c) [188], where each power loss event is represented by blue bars. The effect of the SC bank can be appreciated since, before the commissioning of the ESS, any power losses of more than 4% of the total installed generation capacity would lead to load shedding. Conversely, no load was shed during the SC operation, even though significant generation losses were measured. Due to this excellent performance, the system is expected to be replicated in other markets [188]. Another example of a weak grid is the Yangshan Deep Water Port, near Shanghai, which is located at the end of a 20-mile bridge. The port's 23 quay cranes caused high voltage fluctuations in the grid, while an increase in the transmission line capacity to correct this situation would have involved tremendous cost. A 3 MW, 17.2 kWh supercapacitor storage system was therefore installed to provide 20 seconds of reserve power. This system has been fully operational since 2013 and has led to a 38% reduction in the peak power demand from the grid with no need to upgrade the size of the transmission line [172].

3) INDUSTRIAL SECTOR

Those systems using SCs in the industrial sector include vehicles such as forklifts, shovel trucks, agricultural machinery, excavators, mining shovels, harbor cranes and industrial lasers. SC use in these machines is also stimulated by CO_2 emission regulations imposed in a number of countries. This sector is characterized by long designing and testing periods since they are expensive devices with a small production volume.

Of the machines mentioned above, forklift trucks is the fastest growth segment, since the production volume is much larger than that of other heavier machines. Moreover, the dangers and health concerns related to the indoor use of fossil fuels make all-electric forklifts more common. This kind of vehicle can have either a battery or a fuel cell ESS, and SCs are usually added as a power source to support lifting operations and to recover braking energy [74]. Forklifts of this type have been available on the market for several years. For example, the Komatsu forklift shown in Fig. 19 (a) features a battery – SC storage system and was launched on the market in 2007, as reported in [214]. This kind of system is a current research topic, especially its life cycle analysis [215].

In the harbor crane market, typical characteristics of the energy storage demands include deep discharge cycling. Port cranes equipped with SCs can recover energy from braking and drop manoeuvres, leading to savings on diesel consumption of up to 20% [46]. Extra savings are achieved by reducing the maximum engine power since the peak power is provided by the SC storage system. These systems have shown a 35% reduction in CO_2 emissions. Recent research works on the sizing of ESSs for these applications have been published [216]. The authors of this study compare a battery ESS with an SC – battery hybrid ESS and conclude that the battery – SC hybrid crane shows great potential for regenerative energy recovery associated with a reduction in fuel costs and emissions.

FIGURE 19. Industrial machines that use SCs. FB15HB-12 battery – SC hybrid forklift for Komatsu (a), PC200–8 Hybrid Excavator (b) and Rockster R1100DE Parallel Hybrid Crusher (c). Photos taken from the manufacturers websites.

Earth moving machinery is large sized and mobile, therefore requiring high power peaks. Supercapacitors come within those applications used in combination with diesel motors to meet the high power demand and to recover energy from regenerative movements [74]. Three different hybrid machines are referred to herein as examples of the benefits achieved with SCs. In 2007, Komatsu launched the first hybrid excavator on the market [217], the PC200–8 Hybrid Excavator shown in Fig. 19 (b). Although a diesel engine is the primary energy source of the excavator, an electric motor is used for the turntable of the upper structure. An SC bank is connected to this motor, allowing for energy recovery when the turning slows down. Since the mass of the PC200–8 is 20 100 kg, the SCs allow for energy savings of 25% in standard tests. Real measurements were performed by the manufacturer in a sludge disposal application, where the cabin turns more frequently than in standard tests, and a fuel saving of 41% was recorded [217]. Five years later, in 2012, Caterpillar presented a hybrid hydraulic shovel, the Cat® 6120B H FS, which recovers energy not only from cabin swing deceleration but also from boom-down movements. This energy is stored in SCs, and electric motors are used to assist the diesel engine when maximum power is required. Fuel savings of 25% were also reported [218]. As a final example, the R1100DE Parallel Hybrid Crusher shown in Fig. 19 (c) marketed by Rockster, has the diesel engine directly coupled to a generator. In this way, the engine always operates at its maximum efficiency. Electric motors are used to move the machine, and an SC bank smooths the power peaks required to crush the rocks [219].

4) CONSUMER ELECTRONICS

The consumer electronics segment has a lot of features that make it quite different from the above-mentioned cases. It is costly and time-sensitive for SC manufacturers due to the very short design times and to the significant portion of volume required by the SC in the final device. Although consumer electronics is a very diverse market, the primary uses of SCs in these devices can be classified into four groups, as shown in Fig. 20 [160]:

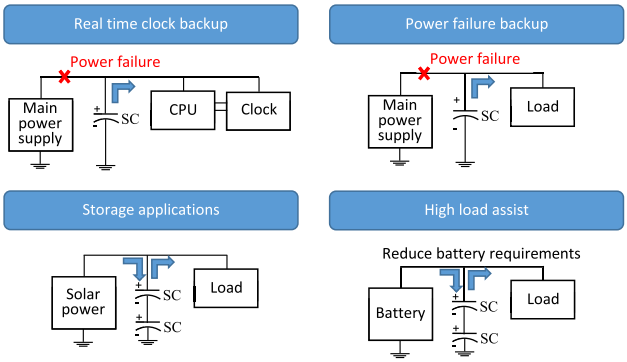

FIGURE 20. Schematic diagram of the use of SCs for different consumer electronic applications.

- Real-time clock or memory backup: for instance, solid-state drives have many advantages over hard-disk drives. However, the write speed is their main weakness, which can be enhanced using protected cache memory (SDRAM). This SDRAM needs a backup power, supplied in many cases by SCs [220].
- Power failure backup: These systems provide emergency power to a load when the primary power source fails. An appropriate backup power supply should be able to provide instantaneous power without glitches. They are typically used to protect hardware such as telecommunication equipment, industrial or other electrical equipment, where an unexpected power disruption can cause malfunction or data loss. Texas Instruments published a report [221] in which the performance of a backup power supply which uses SCs as an ESS is analyzed in detail.
- Storage applications in which SCs are used instead of batteries: The fast charging capability, long lifetime and low maintenance requirements make SCs more advantageous than batteries as an ESS for some devices. Two examples of these applications are a flashlight with SC energy storage [222] and a solar energy harvesting system using SCs as ESS [223].

- High load assist to the primary ESS: In some applications, such as the flash of a smartphone camera, the peak power load is significantly higher, albeit for a short time, than that of any other use case. SCs are selected as secondary power sources in order to use a low-power, cheaper battery as the primary source of energy. Several manufacturers have been using SCs for a number of years, such as the IC presented by STMicroelectronics in 2012, which is an integrated camera flash controller combining a supercapacitor, a discrete high-current MOSFET switch and high-power white LEDs [224].

VI. SUMMARY AND OUTLOOK

As detailed in this review, SCs are an energy storage technology which is of increasing interest due to the growing need for robust ESSs able to manage high power peaks. This paper provides a broad overview of the technology with particular focus on the electrical characteristics and applications. To do so, SCs are firstly compared with other storage technologies and are identified as devices that bridge the gap between batteries and conventional capacitors with regard to power and energy density. The physical principles that are the basis of SC performance (double layer, pseudocapacitance and faradaic processes) are also explained based on research papers published on these topics, while some misused terms and mistaken concepts are identified and clarified. These physical principles are then related to the electrical characteristics derived from each one, which is of particular interest for an optimal application of SCs in electrical systems. Subsequently, a compilation is made of the most promising materials used as electrodes and electrolytes, proposing a classification of the SCs based on these materials and also describing the electrical implications of the material properties.

A detailed analysis of the most noteworthy electrical phenomena observable in an SC is then presented. In this regard, capacitance and differential capacitance are described, and the difference between both parameters is clarified. The implications of charge distribution mechanisms along the electrode surface are covered, as well as the ohmic phenomena, which entail a voltage drop proportional to current. Electrical self-discharge and the high-frequency operation of SCs are also analyzed based on their implications on SC performance. Given the importance of energy and power density for the analysis of ESSs, these two concepts are detailed and sensible expressions used in the literature to particularize their calculation for SCs are stated.

The most common modeling approaches are summarized in this review. The starting point is models based on electrochemical phenomena, which are the historical origin of the understanding of SCs. This is followed by a summary of the most important molecular modeling ideas, given the importance of these models for the SC design and manufacturing process. The next modeling trend is that of electrical circuit models, which are divided into transmission-line models, fractional models, and simplified analytical models, which are electrical circuit models obtained by the simplification of physical equations. Finally, thermal modeling is also covered and the importance of thermal management for the safe performance and long lifetime of SCs is highlighted. In addition to the most important recent ideas related to each of these model approaches, some future research topics are highlighted, and experimental procedures for the characterization of the SC behavior, analyzed by each modeling technique, are critically described.

Finally, the SC manufacturing process is summarized, and the differences between the two most common products (cylindrical and pouch supercapacitors) are analyzed. A table with the key features of commercial products is provided, and the applications suggested by the manufacturers are also addressed. An analysis of the current SC market divided into its four sectors (transport, energy, industrial and consumer electronics) is presented with recent examples of successful engineering applications in which SCs play a key role as ESSs, as well as research papers in which improvements and new ideas for these needs are proposed.

The SC market is experiencing a remarkable expansion, which needs to be accompanied by intensive research and development at several levels aimed at enhancing their energy density and reducing cost while maintaining high power, safe and long working life. The most promising research trends on the topics analyzed through the paper are addressed hereafter. Firstly, material improvements, both in electrodes and electrolytes are expected in the next few years. The cost of the electrodes represent 40–65% of the total SC cost. Therefore, the development of new high surface carbon compounds obtained from biological sources, which avoid the costly high temperature processes, such as carbon activation, can bring important reductions of SC costs. Moreover, the currently-used expensive substrates used to reach reasonable energy density on graphene electrodes need to be researched towards cheaper alternatives. For pseudocapacitors, which can offer a good power–energy–cost–life balance in the near future, new electrode materials with lower cost and higher performance need to be achieved. Metal oxides are seen as a promising research trend in this line. With regard to electrolytes, there is a new drive towards the widening of the decomposition voltage window for aqueous electrolytes and to lower costs and higher ion mobility in ionic liquids in order to compete against organic electrolytes. The manufacturing process also needs to be improved by the designing of new techniques that allow for a better control of the pore size in the micro- and meso-scale that are scalable to the big electrode size required for mass production. Moreover, the technology needed for the production of flexible SCs, which could be of considerable interest during the upcoming years, is also to be developed.

The engineering design of energy systems with SCs needs to be updated in order to achieve the best results from current technology, and two trends need to be considered for a successful design: (*i*) for designs where low cost, low maintenance and long life compensate for low energy density

and moderate power density, aqueous asymmetric systems are the best option, while (*ii*) for designs where high power has a main importance and compensates for higher cost and low energy density, organic symmetric SCs are usually preferred. Finally, the expected lifetime of an SC is set to grow in upcoming years. Thus, the understanding and modeling of ageing mechanisms for different devices and the design of control strategies to minimize this effect are taking on increasing importance.

The high power capability, exceptional efficiency, decreasing price, ability to operate in hostile environments, low maintenance requirements and long lifetime offered by SCs are making this technology a desirable option for the increasing number of electrical applications requiring an outstanding ESS.

REFERENCES

[1] M. Aneke and M. Wang, "Energy storage technologies and real life applications—A state of the art review," *Appl. Energy*, vol. 179, pp. 350–377, Oct. 2016.

[2] J. Li, G. Zhang, C. Fu, L. Deng, R. Sun, and C.-P. Wong, "Facile preparation of nitrogen/sulfur co-doped and hierarchical porous graphene hydrogel for high-performance electrochemical capacitor," *J. Power Sources*, vol. 345, pp. 146–155, Mar. 2017.

[3] K. Parida, V. Bhavanasi, V. Kumar, J. Wang, and P. S. Lee, "Fast charging self-powered electric double layer capacitor," *J. Power Sources*, vol. 342, pp. 70–78, Feb. 2017.

[4] L. Zhang, Z. Wang, X. Hu, F. Sun, and D. G. Dorrell, "A comparative study of equivalent circuit models of ultracapacitors for electric vehicles," *J. Power Sources*, vol. 274, no. 8, pp. 899–906, 2015.

[5] P. Sharma and T. S. Bhatti, "A review on electrochemical double-layer capacitors," *Energy Convers. Manage.*, vol. 51, no. 12, pp. 2901–2912, 2010.

[6] W. Münchgesang, P. Meisner, G. Yushin, D. C. Meyer, and T. Leisegang, "Supercapacitors specialities—Technology review," in *Proc. AIP Conf.*, vol. 1597, no. 1, 2014, pp. 196–203.

[7] A. González, E. Goikolea, J. A. Barrena, and R. Mysyk, "Review on supercapacitors: Technologies and materials," *Renew. Sustain. Energy Rev.*, vol. 58, pp. 1189–1206, May 2016.

[8] C. Zhong, Y. Deng, W. Hu, J. Qiao, L. Zhang, and J. Zhang, "A review of electrolyte materials and compositions for electrochemical supercapacitors," *Chem. Soc. Rev.*, vol. 44, no. 21, pp. 7484–7539, 2015.

[9] Y. Wang, Y. Song, and Y. Xia, "Electrochemical capacitors: Mechanism, materials, systems, characterization and applications," *Chem. Soc. Rev.*, vol. 45, no. 21, pp. 5925–5950, 2016.

[10] S. Zhang and N. Pan, "Supercapacitors performance evaluation," *Adv. Energy Mater.*, vol. 5, no. 6, p. 1401, 2015.

[11] L. Zhang, X. Hu, Z. Wang, F. Sun, and D. Dorrell, "A review of supercapacitor modeling, estimation, and applications: A control/management perspective," *Renew. Sustain. Energy Rev.*, vol. 81, no. 2, pp. 1868–1878, Jan. 2018.

[12] A. Muzaffar, M. B. Ahamed, K. Deshmukh, and J. Thirumalai, "A review on recent advances in hybrid supercapacitors: Design, fabrication and applications," *Renew. Sustain. Energy Rev.*, vol. 101, pp. 123–145, Mar. 2019.

[13] S. Faraji and F. N. Ani, "The development supercapacitor from activated carbon by electroless plating—A review," *Renew. Sustain. Energy Rev.*, vol. 42, pp. 823–834, Feb. 2015.

[14] B. E. Conway, *Electrochemical Supercapacitors: Scientific Fundamentals and Technological Applications*. New York, NY, USA: Academic, 1999.

[15] P. Simon, Y. Gogotsi, and B. Dunn, "Where do batteries end and supercapacitors begin?" *Science*, vol. 343, no. 6176, pp. 1210–1211, 2014.

[16] A. Ursúa and P. Sanchis, "Static–dynamic modelling of the electrical behaviour of a commercial advanced alkaline water electrolyser," *Int. J. Hydrogen Energy*, vol. 37, no. 24, pp. 18598–18614, 2012.

[17] I. S. Martín, A. Ursúa, and P. Sanchis, "Modelling of PEM fuel cell performance: Steady-state and dynamic experimental validation," *Energies*, vol. 7, no. 2, pp. 670–700, 2014.

[18] A. Berrueta, V. Irigaray, P. Sanchis, and A. Ursúa, "Lithium-ion battery model and experimental validation," in *Proc. 17th Eur. Conf. Power Electron. Appl. (EPE ECCE-Europe)*, Sep. 2015, pp. 1–8.

[19] G. Pilatowicz *et al.*, "Determination of the lead-acid battery's dynamic response using Butler-Volmer equation for advanced battery management systems in automotive applications," *J. Power Sources*, vol. 331, pp. 348–359, Nov. 2016.

[20] T. Broussea, D. Bélangerc, and J. W. Long, "To be or not to be pseudocapacitive?," *J. Electrochem. Soc.*, vol. 162, no. 5, pp. A5185–A5189, 2015.

[21] S. Trasatti and G. Buzzanca, "Ruthenium dioxide: A new interesting electrode material. Solid state structure and electrochemical behaviour," *J. Electroanal. Chem. Interfacial Electrochem.*, vol. 29, pp. A1–A5, Feb. 1971.

[22] O. Ghodbane, F. Ataherian, N.-L. Wu, and F. Favier, "*In situ* crystallographic investigations of charge storage mechanisms in MnO_2-based electrochemical capacitors," *J. Power Sources*, vol. 206, pp. 454–462, May 2012.

[23] Y. Zeng, M. Yu, Y. Meng, P. Fang, X. Lu, and Y. Tong, "Iron-based supercapacitor electrodes: Advances and challenges," *Adv. Energy Mater.*, vol. 6, no. 24, 2016, Art. no. 1601053.

[24] H. Xu, X. Hu, H. Yang, Y. Sun, C. Hu, and Y. Huang, "Flexible asymmetric micro-supercapacitors based on Bi_2O_3 and MnO_2 nanoflowers: Larger areal mass promises higher energy density," *Adv. Energy Mater.*, vol. 5, no. 6, 2015, Art. no. 1401882.

[25] Y. Zeng *et al.*, "Advanced Ti-doped Fe_2O_3@PEDOT core/shell anode for high-energy asymmetric supercapacitors," *Adv. Energy Mater.*, vol. 5, no. 12, 2015, Art. no. 1402176.

[26] J. Li *et al.*, "Achieving high pseudocapacitance of 2D titanium carbide (MXene) by cation intercalation and surface modification," *Adv. Energy Mater.*, vol. 7, no. 15, 2017, Art. no. 1602725.

[27] N. Kurra, Q. Jiang, A. Syed, C. Xia, and H. N. Alshareef, "Micro-pseudocapacitors with electroactive polymer electrodes: Toward AC-line filtering applications," *Appl. Mater. Interfaces*, vol. 8, no. 20, pp. 12748–12755, 2016.

[28] A. Eftekhari, L. Li, and Y. Yang, "Polyaniline supercapacitors," *J. Power Sources*, vol. 347, pp. 86–107, Apr. 2017.

[29] L. Wang *et al.*, "*In situ* preparation of SnO_2@polyaniline nanocomposites and their synergetic structure for high-performance supercapacitors," *J. Mater. Chem. A*, vol. 2, no. 22, pp. 8334–8341, 2014.

[30] L. Li *et al.*, "High-performance pseudocapacitive microsupercapacitors from laser-induced graphene," *Adv. Mater.*, vol. 28, no. 5, pp. 838–845, 2016.

[31] A. Eftekhari and H. García, "The necessity of structural irregularities for the chemical applications of graphene," *Mater. Chem. Today*, vol. 4, pp. 1–16, Jun. 2017.

[32] A. Eftekhari and F. Molaei, "Carbon nanotube-assisted electrodeposition. Part I: Battery performance of manganese oxide films electrodeposited at low current densities," *J. Power Sources*, vol. 274, pp. 1306–1314, Jan. 2015.

[33] A. Eftekhari and F. Molaei, "Carbon nanotube-assisted electrodeposition. Part II: Superior pseudo-capacitive behavior of manganese oxide film electrodeposited at high current densities," *J. Power Sources*, vol. 274, pp. 1315–1321, Jan. 2015.

[34] I. Hadjipaschalis, A. Poullikkas, and V. Efthimiou, "Overview of current and future energy storage technologies for electric power applications," *Renew. Sustain. Energy Rev.*, vol. 13, nos. 6–7, pp. 1513–1522, 2009.

[35] C. Lei and C. Lekakou, "Carbon-based nanocomposite EDLC supercapacitors," in *Proc. Nanotech Conf. Expo*, vol. 1, 2010, pp. 176–179.

[36] R. Emmett *et al.*, "Can faradaic processes in residual iron catalyst help overcome intrinsic EDLC limits of carbon nanotubes?" *J. Phys. Chem. C*, vol. 118, no. 46, pp. 26498–26503, 2014.

[37] S. Kwon, B.-S. Kim, S.-G. Kim, B.-J. Lee, M.-S. Kim, and J. Jung, "Preparation of nano-porous activated carbon aerogel using a single-step activation method for use as high-power EDLC electrode in organic electrolyte," *J. Nanosci. Nanotechnol.*, vol. 16, no. 5, pp. 4598–4604, 2016.

[38] H. Seo, S.-G. Kim, J. Jung, and M.-S. Kim, "Preparation and characterization of carbon aerogel activated with KOH and CO_2: Effect of pore size distribution on electrochemical properties as EDLC electrodes," *Polymer*, vol. 40, no. 4, pp. 577–586, 2016.

[39] S. Ye, L. Zhu, I.-J. Kim, S.-H. Yang, and W.-C. Oh, "Characterization of expanded graphene nanosheet as additional material and improved performances for electric double layer capacitors," *J. Ind. Eng. Chem.*, vol. 43, pp. 53–60, Nov. 2016.
[40] Y. Maletin *et al.*, "Electrochemical double layer capacitors and hybrid devices for green energy applications," *Green*, vol. 4, nos. 1–6, pp. 9–17, 2014.
[41] Z.-S. Wu, W. Ren, D.-W. Wang, F. Li, B. Liu, and H.-M. Cheng, "High-energy MnO_2 nanowire/graphene and graphene asymmetric electrochemical capacitors," *ACS Nano*, vol. 4, no. 10, pp. 5835–5842, 2010.
[42] C. Liu, C. Zhang, H. Fu, X. Nan, and G. Cao, "Exploiting high-performance anode through tuning the character of chemical bonds for Li-ion batteries and capacitors," *Adv. Energy Mater.*, vol. 7, no. 1, 2017, Art. no. 1601127.
[43] F. Zhang *et al.*, "A high-performance supercapacitor-battery hybrid energy storage device based on graphene-enhanced electrode materials with ultrahigh energy density," *Energy Environ. Sci.*, vol. 6, no. 5, pp. 1623–1632, 2013.
[44] VINATech. *Supercapacitor Solution*. Accessed: Jan. 2019. [Online]. Available: http://www.vina.co.kr/eng/product/supercap.html
[45] Yunasko. *Ultracapacitor Product Line*. Accessed: Jan. 2019. [Online]. Available: http://yunasko.com/en/products
[46] Maxwell Technologies. *Maxell Ultracapacitors*. Accessed: Feb. 2019. [Online]. Available: http://www.maxwell.com/products/ultracapacitors/
[47] D. Chen, Q. Wang, R. Wang, and G. Shen, "Ternary oxide nanostructured materials for supercapacitors: A review," *J. Mater. Chem. A*, vol. 3, no. 19, pp. 10158–10173, 2015.
[48] L. O'Neill, C. Johnston, and P. S. Grant, "Enhancing the supercapacitor behaviour of novel Fe_3O_4/FeOOH nanowire hybrid electrodes in aqueous electrolytes," *J. Power Sources*, vol. 274, pp. 907–915, Jan. 2015.
[49] W. Zhang, Y. H. Qu, and L. J. Gao, "Performance of PbO_2/activated carbon hybrid supercapacitor with carbon foam substrate," *Chin. Chem. Lett.*, vol. 23, no. 5, pp. 623–626, 2012.
[50] M. Soumya *et al.*, "Electrochemical performance of PbO_2 and PbO_2–CNT composite electrodes for energy storage devices," *J. Nanosci. Nanotechnol.*, vol. 15, no. 1, pp. 703–708, 2015.
[51] W. Sun, X. Rui, M. Ulaganathan, S. Madhavi, and Q. Yan, "Few-layered $Ni(OH)_2$ nanosheets for high-performance supercapacitors," *J. Power Sources*, vol. 295, pp. 323–328, Nov. 2015.
[52] J. Zhu, W. Zu, G. Yang, and Q. Song, "A novel electrochemical supercapacitor based on $Li_4Ti_5O_12$ and $LiNi_{1/3}Co_{1/3}Mn_{1/3}O_2$," *Mater. Lett.*, vol. 115, pp. 237–240, Jan. 2014.
[53] J. Li, J. Guo, X. Zhang, Y. Huang, and L. Guo, "Asymmetric supercapacitors with high energy and power density fabricated using $LiMn_2O_4$ nanorods and activated carbon electrodes," *Int. J. Electrochem. Sci.*, vol. 12, no. 2, pp. 1157–1166, 2017.
[54] H. Liu, L. Liao, Y.-C. Lu, and Q. Li, "High energy density aqueous Li-ion flow capacitor," *Adv. Energy Mater.*, vol. 7, no. 1, 2017, Art. no. 1601248.
[55] B. Li *et al.*, "Activated carbon from biomass transfer for high-energy density lithium-ion supercapacitors," *Adv. Energy Mater.*, vol. 6, no. 18, 2016, Art. no. 1600802.
[56] W. Gu and G. Yushin, "Review of nanostructured carbon materials for electrochemical capacitor applications: Advantages and limitations of activated carbon, carbide-derived carbon, zeolite-templated carbon, carbon aerogels, carbon nanotubes, onion-like carbon, and graphene," *Wiley Interdiscipl. Rev., Energy Environ.*, vol. 3, no. 5, pp. 424–473, 2014.
[57] A. Balducci, "Electrolytes for high voltage electrochemical double layer capacitors: A perspective article," *J. Power Sources*, vol. 326, pp. 534–540, Sep. 2016.
[58] R. Burt, G. Birkett, and X. S. Zhao, "A review of molecular modelling of electric double layer capacitors," *Phys. Chem. Chem. Phys.*, vol. 16, no. 14, pp. 6519–6538, 2014.
[59] C. Schütter, T. Husch, V. Viswanathan, S. Passerini, A. Balducci, and M. Korth, "Rational design of new electrolyte materials for electrochemical double layer capacitors," *J. Power Sources*, vol. 326, pp. 541–548, Sep. 2016.
[60] K. Soeda, M. Yamagata, S. Yamazaki, and M. Ishikawa, "Application of chitosan-based gel electrolytes with ionic liquids for high-performance and safe electric double layer capacitors," *Electrochemistry*, vol. 81, no. 10, pp. 867–872, 2013.
[61] K. Fic, G. Lota, M. Meller, and E. Frackowiak, "Novel insight into neutral medium as electrolyte for high-voltage supercapacitors," *Energy Environ. Sci.*, vol. 5, no. 2, pp. 5842–5850, 2012.
[62] C. Hu, E. Zhao, N. Nitta, A. Magasinski, G. Berdichevsky, and G. Yushin, "Aqueous solutions of acidic ionic liquids for enhanced stability of polyoxometalate-carbon supercapacitor electrodes," *J. Power Sources*, vol. 326, pp. 569–574, Sep. 2016.
[63] A. Eftekhari, "Supercapacitors utilising ionic liquids," *Energy Storage Mater.*, vol. 9, pp. 47–69, Oct. 2017.
[64] M. Cowell, R. Winslow, Q. Zhang, J. Ju, J. Evans, and P. Wright, "Composite carbon-based ionic liquid supercapacitor for high-current micro devices," *J. Phys., Conf. Ser.*, vol. 557, no. 1, 2014, Art. no. 012061.
[65] X. Lyu, F. Su, and M. Miao, "Two-ply yarn supercapacitor based on carbon nanotube/stainless steel core-sheath yarn electrodes and ionic liquid electrolyte," *J. Power Sources*, vol. 307, pp. 489–495, Mar. 2016.
[66] M. Buzzeo, R. Evans, and R. Compton, "Non-haloaluminate room-temperature ionic liquids in electrochemistry—A review," *ChemPhysChem*, vol. 5, no. 8, pp. 1106–1120, 2004.
[67] L. Zhang, K. Tsay, C. Bock, and J. Zhang, "Ionic liquids as electrolytes for non-aqueous solutions electrochemical supercapacitors in a tempeature range of 20 °C–80 °C," *J. Power Sources*, vol. 324, pp. 615–624, Aug. 2016.
[68] J. G. Huddleston *et al.*, "Characterization and comparison of hydrophilic and hydrophobic room temperature ionic liquids incorporating the imidazolium cation," *Green Chem.*, vol. 3, no. 4, pp. 156–164, 2001.
[69] S. Aparicio, M. Atilhan, and F. Karadas, "Thermophysical properties of pure ionic liquids: Review of present situation," *Ind. Eng. Chem. Res.*, vol. 49, no. 20, pp. 9580–9595, 2010.
[70] K. Liu and J. Wu, "Boosting the performance of ionic-liquid-based supercapacitors with polar additives," *J. Phys. Chem. C*, vol. 120, no. 42, pp. 24041–24047, 2016.
[71] S. Pohlmann, T. Olyschläger, P. Goodrich, J. A. Vicente, J. Jacquemin, and A. Balducci, "Mixtures of azepanium based ionic liquids and propylene carbonate as high voltage electrolytes for supercapacitors," *Electrochim. Acta*, vol. 153, pp. 426–432, Jan. 2015.
[72] A. R. Neale *et al.*, "An ether-functionalised cyclic sulfonium based ionic liquid as an electrolyte for electrochemical double layer capacitors," *J. Power Sources*, vol. 326, pp. 549–559, 2016.
[73] A. M. Obeidat, M. A. Gharaibeh, and M. Obaidat, "Solid-state supercapacitors with ionic liquid gel polymer electrolyte and polypyrrole electrodes for electrical energy storage," *J. Energy Storage*, vol. 13, pp. 123–128, Oct. 2017.
[74] J. Miller, *Ultracapacitor Applications* (Energy Engineering). Edison, NJ, USA: IET, 2011.
[75] S. Vaquero, R. Díaz, M. Anderson, J. Palma, and R. Marcilla, "Insights into the influence of pore size distribution and surface functionalities in the behaviour of carbon supercapacitors," *Electrochim. Acta*, vol. 86, pp. 241–247, Dec. 2012.
[76] J. Rouquerol *et al.*, "Recommendations for the characterization of porous solids," *Pure Appl. Chem.*, vol. 66, no. 8, pp. 1739–1758, 1994.
[77] X. B. Xiong, J. Y. Zhang, J. Ma, X. R. Zeng, H. Qian, and Y. Y. Li, "Fabrication of porous nickel (hydr)oxide film with rational pore size distribution on nickel foam by induction heating deposition for high-performance supercapacitors," *Mater. Chem. Phys.*, vol. 181, pp. 1–6, Sep. 2016.
[78] D. Tang *et al.*, "Self-templated synthesis of mesoporous carbon from carbon tetrachloride precursor for supercapacitor electrodes," *ACS Appl. Mater. Interfaces*, vol. 8, no. 11, pp. 6779–6783, 2016.
[79] I. Yang, S.-G. Kim, S. H. Kwon, J. H. Lee, M.-S. Kim, and J. C. Jung, "Pore size-controlled carbon aerogels for EDLC electrodes in organic electrolytes," *Current Appl. Phys.*, vol. 16, no. 6, pp. 665–672, 2016.
[80] N. Bhandari, R. Dua, L. Estevez, R. Sahore, and E. P. Giannelis, "A combined salt–hard templating approach for synthesis of multi-modal porous carbons used for probing the simultaneous effects of porosity and electrode engineering on EDLC performance," *Carbon*, vol. 87, pp. 29–43, Jun. 2015.
[81] M. Kunowsky, C. Linares-Solano, A. Garcia-Gomez, V. Barranco, J. M. Rojo, and J. D. Carruthers, "Applications for CO_2-activated carbon monoliths: II. EDLC electrodes," *Int. J. Appl. Ceram. Technol.*, vol. 12, pp. E127–E132, Jan. 2015.
[82] Y. Zhu *et al.*, "Carbon-based supercapacitors produced by activation of graphene," *Science*, vol. 332, no. 6037, pp. 1537–1541, Jun. 2011.
[83] A. Berrueta, I. S. Martín, A. Hernández, A. Ursúa, and P. Sanchis, "Electro-thermal modelling of a supercapacitor and experimental validation," *J. Power Sources*, vol. 259, pp. 154–165, Aug. 2014.

[84] L. Zubieta and R. Bonert, "Characterization of double-layer capacitors for power electronics applications," *IEEE Trans. Ind. Appl.*, vol. 36, no. 1, pp. 199–205, Jan. 2000.
[85] W. Lajnef, J.-M. Vinassa, O. Briat, S. Azzopardi, and E. Woirgard, "Characterization methods and modelling of ultracapacitors for use as peak power sources," *J. Power Sources*, vol. 168, no. 2, pp. 553–560, 2007.
[86] E. J. Brandon, W. C. West, M. C. Smart, L. D. Whitcanack, and G. A. Plett, "Extending the low temperature operational limit of double-layer capacitors," *J. Power Sources*, vol. 170, no. 1, pp. 225–232, 2007.
[87] H. Gualous, D. Bouquain, A. Berthon, and J. M. Kauffmann, "Experimental study of supercapacitor serial resistance and capacitance variations with temperature," *J. Power Sources*, vol. 123, no. 1, pp. 86–93, 2003.
[88] H. Michel, "Temperature and dynamics problems of ultracapacitors in stationary and mobile applications," *J. Power Sources*, vol. 154, no. 2, pp. 556–560, 2006.
[89] B. Daffos, P.-L. Taberna, Y. Gogotsi, and P. Simon, "Recent advances in understanding the capacitive storage in microporous carbons," *Fuel Cells*, vol. 10, no. 5, pp. 819–824, 2010.
[90] S. I. Fletcher *et al.*, "The effects of temperature on the performance of electrochemical double layer capacitors," *J. Power Sources*, vol. 195, no. 21, pp. 7484–7488, 2010.
[91] J. Torres, pp. Moreno–Torres, G. Navarro, M. Blanco, and M. Lafoz, "Fast energy storage systems comparison in terms of energy efficiency for a specific application," *IEEE Access*, vol. 6, pp. 40656–40672, 2018.
[92] D. Mishra and S. De, "Effects of practical rechargeability constraints on perpetual RF harvesting sensor network operation," *IEEE Access*, vol. 4, pp. 750–765, 2016.
[93] B. Ricketts and C. Ton-That, "Self-discharge of carbon-based supercapacitors with organic electrolytes," *J. Power Sources*, vol. 89, no. 1, pp. 64–69, Jul. 2000.
[94] C. Hao, X. Wang, Y. Yin, and Z. You, "Analysis of charge redistribution during self-discharge of double-layer supercapacitors," *J. Electron. Mater.*, vol. 45, no. 4, pp. 2160–2171, 2016.
[95] J.-F. Shen, Y.-J. He, and Z.-F. Ma, "A systematical evaluation of polynomial based equivalent circuit model for charge redistribution dominated self-discharge process in supercapacitors," *J. Power Sources*, vol. 303, pp. 294–304, Jan. 2016.
[96] V. R. S. Visentini, L. M. C. Zarpelon, and R. N. Faria, "Self-discharge and microstructure of supercapacitors tested at room temperature and at 333 K," *Mater. Sci. Forum*, vol. 802, pp. 427–432, Dec. 2014.
[97] S. Fletcher, V. J. Black, and I. Kirkpatrick, "A universal equivalent circuit for carbon-based supercapacitors," *J. Solid State Electrochem.*, vol. 18, no. 5, pp. 1377–1387, 2014.
[98] T. Tevi, H. Yaghoubi, J. Wang, and A. Takshi, "Application of poly (p-phenylene oxide) as blocking layer to reduce self-discharge in supercapacitors," *J. Power Sources*, vol. 241, pp. 589–596, Nov. 2013.
[99] T. Tevi and A. Takshi, "Modeling and simulation study of the self-discharge in supercapacitors in presence of a blocking layer," *J. Power Sources*, vol. 273, pp. 857–862, Jan. 2015.
[100] H. Yang and Y. Zhang, "A task scheduling algorithm based on supercapacitor charge redistribution and energy harvesting for wireless sensor nodes," *J. Energy Storage*, vol. 6, pp. 186–194, May 2016.
[101] F. Rafik, H. Gualous, R. Gallay, A. Crausaz, and A. Berthon, "Frequency, thermal and voltage supercapacitor characterization and modeling," *J. Power Sources*, vol. 165, no. 2, pp. 928–934, Mar. 2007.
[102] J. R. Miller, R. A. Outlaw, and B. C. Holloway, "Graphene double-layer capacitor with ac line-filtering performance," *Science*, vol. 329, no. 5999, pp. 1637–1639, 2010.
[103] H. Helmholtz, "Studien über electrische Grenzschichten," *Ann. Phys.*, vol. 243, no. 7, pp. 337–382, 1879.
[104] H. Wang and L. Pilon, "Accurate simulations of electric double layer capacitance of ultramicroelectrodes," *J. Phys. Chem. C*, vol. 115, no. 33, pp. 16711–16719, 2011.
[105] A. J. Bard and L. R. Faulkner, *Electrochemical Methods: Fundamentals and Applications*. Hoboken, NJ, USA: Wiley, 2001.
[106] G. Guoy, "Constitution of the electric charge at the surface of an electrolyte," *J. Phys.*, vol. 9, no. 1, pp. 67–457, 1910.
[107] D. L. Chapman, "LI. A contribution to the theory of electrocapillarity," *London, Edinburgh, Dublin Philos. Mag. J. Sci.*, vol. 25, no. 148, pp. 475–481, 1913.
[108] O. Stern, "The theory of the electrolytic double–layer," *Z. Elektrochem*, vol. 30, no. 508, pp. 1014–1020, 1924.
[109] V. Srinivasan and J. W. Weidner, "Mathematical modeling of electrochemical capacitors," *J. Electrochem. Soc.*, vol. 146, no. 5, pp. 1650–1658, 1999.
[110] R. Drummond, D. A. Howey, and S. R. Duncan, "Low-order mathematical modelling of electric double layer supercapacitors using spectral methods," *J. Power Sources*, vol. 277, pp. 317–328, Mar. 2015.
[111] M. P. Allen and D. J. Tildesley, *Computer Simulation of Liquids*. London, U.K.: Oxford Univ. Press, 1989.
[112] D. Frenkel and B. Smit, *Understanding Molecular Simulation: From Algorithms to Applications*, vol. 1. New York, NY, USA: Academic, 2001.
[113] Y. Wang, W. Jiang, T. Yan, and G. A. Voth, "Understanding ionic liquids through atomistic and coarse-grained molecular dynamics simulations," *Accounts Chem. Res.*, vol. 40, no. 11, pp. 1193–1199, 2007.
[114] A. Mundy and G. L. Plett, "Reduced-order physics-based modeling and experimental parameter identification for non-faradaic electrical double-layer capacitors," *J. Energy Storage*, vol. 7, pp. 167–180, Aug. 2016.
[115] J. Vatamanu, O. Borodin, and G. D. Smith, "Molecular insights into the potential and temperature dependences of the differential capacitance of a room-temperature ionic liquid at graphite electrodes," *J. Amer. Chem. Soc.*, vol. 132, no. 42, pp. 14825–14833, 2010.
[116] L. Xing, J. Vatamanu, O. Borodin, and D. Bedrov, "On the atomistic nature of capacitance enhancement generated by ionic liquid electrolyte confined in subnanometer pores," *J. Phys. Chem. Lett.*, vol. 4, no. 1, pp. 132–140, 2012.
[117] S. Li *et al.*, "Molecular dynamics simulation study of the capacitive performance of a binary mixture of ionic liquids near an onion-like carbon electrode," *J. Phys. Chem. Lett.*, vol. 3, no. 17, pp. 2465–2469, 2012.
[118] E. Paek, A. J. Pak, and G. S. Hwang, "A computational study of the interfacial structure and capacitance of graphene in [BMIM][PF_6] ionic liquid," *J. Electrochem. Soc.*, vol. 160, no. 1, pp. A1–A10, 2013.
[119] C. Merlet, C. Péan, B. Rotenberg, P. A. Madden, P. Simon, and M. Salanne, "Simulating supercapacitors: Can we model electrodes as constant charge surfaces?" *J. Phys. Chem. Lett.*, vol. 4, no. 2, pp. 264–268, 2012.
[120] J. Griffin, A. C. Forse, W.-Y. Tsai, P.-L. Taberna, P. Simon, and C. P. Grey, "*In situ* NMR and electrochemical quartz crystal microbalance techniques reveal the structure of the electrical double layer in supercapacitors," *Nature Mater.*, vol. 14, no. 8, pp. 812–819, 2015.
[121] D. Torregrossa, K. E. Toghill, V. Amstutz, H. H. Girault, and M. Paolone, "Macroscopic indicators of fault diagnosis and ageing in electrochemical double layer capacitors," *J. Energy Storage*, vol. 2, pp. 8–24, Aug. 2015.
[122] S. Kumagai, K. Mukaiyachi, and D. Tashima, "Rate and cycle performances of supercapacitors with different electrode thickness using non-aqueous electrolyte," *J. Energy Storage*, vol. 3, pp. 10–17, Oct. 2015.
[123] R. de Levie, "On porous electrodes in electrolyte solutions: I. Capacitance effects," *Electrochim. Acta*, vol. 8, no. 10, pp. 751–780, 1963.
[124] R. de Levie, "On the impedance of electrodes with rough interfaces," *J. Electroanal. Chem. Interfacial Electrochem.*, vol. 261, no. 1, pp. 1–9, 1989.
[125] C. Pean, B. Rotenberg, P. Simon, and M. Salanne, "Multi-scale modelling of supercapacitors: From molecular simulations to a transmission line model," *J. Power Sources*, vol. 326, pp. 680–685, Sep. 2016.
[126] S. Moayedi, F. Cingoz, and A. Davoudi, "Accelerated simulation of high-fidelity models of supercapacitors using waveform relaxation techniques," *IEEE Trans. Power Electron.*, vol. 28, no. 11, pp. 4903–4909, Nov. 2013.
[127] P.-O. Logerais *et al.*, "Modeling of a supercapacitor with a multibranch circuit," *Int. J. Hydrogen Energy*, vol. 40, no. 39, pp. 13725–13736, 2015.
[128] A. Ghosh, V. T. Le, J. J. Bae, and Y. H. Lee, "TLM-PSD model for optimization of energy and power density of vertically aligned carbon nanotube supercapacitor," *Sci. Rep.*, vol. 3, Oct. 2013, Art. no. 2939.
[129] R. Gonçalves, W. Christinelli, A. Trench, A. Cuesta, and E. Pereira, "Properties improvement of poly (o-methoxyaniline) based supercapacitors: Experimental and theoretical behaviour study of self-doping effect," *Electrochim. Acta*, vol. 228, pp. 57–65, Feb. 2017.
[130] J. P. Meyers, M. Doyle, R. M. Darling, and J. Newman, "The impedance response of a porous electrode composed of intercalation particles," *J. Electrochem. Soc.*, vol. 147, no. 8, pp. 2930–2940, 2000.
[131] R. Drummond, S. Zhao, D. A. Howey, and S. R. Duncan, "Circuit synthesis of electrochemical supercapacitor models," *J. Energy Storage*, vol. 10, pp. 48–55, Apr. 2017.
[132] N. Devillers, S. Jemei, M.-C. Péra, D. Bienaimé, and F. Gustin, "Review of characterization methods for supercapacitor modelling," *J. Power Sources*, vol. 246, pp. 596–608, Jan. 2014.

[133] H. Miniguano, A. Barrado, C. Raga, A. Lázaro, C. Fernández, and M. Sanz, "A comparative study and parameterization of electrical battery models applied to hybrid electric vehicles," in *Proc. Int. Conf. Electr. Syst. Aircr., Railway, Ship Propuls. Road Vehicles Int. Transp. Electrific. Conf. (ESARS-ITEC)*, Nov. 2016, pp. 1–6.
[134] C.-T. Goh and A. Cruden, "Bivariate quadratic method in quantifying the differential capacitance and energy capacity of supercapacitors under high current operation," *J. Power Sources*, vol. 265, pp. 291–298, Nov. 2014.
[135] R. L. Spyker and R. M. Nelms, "Classical equivalent circuit parameters for a double-layer capacitor," *IEEE Trans. Aerosp. Electron. Syst.*, vol. 36, no. 3, pp. 829–836, Jul. 2000.
[136] A. Eddahech, M. Ayadi, O. Briat, and J.-M. Vinassa, "Online parameter identification for real-time supercapacitor performance estimation in automotive applications," *Int. J. Electr. Power Energy Syst.*, vol. 51, no. 1, pp. 162–167, Oct. 2013.
[137] S. Fletcher, I. Kirkpatrick, R. Dring, R. Puttock, R. Thring, and S. Howroyd, "The modelling of carbon-based supercapacitors: Distributions of time constants and Pascal equivalent circuits," *J. Power Sources*, vol. 345, pp. 247–253, Mar. 2017.
[138] V. Sedlakova *et al.*, "Supercapacitor equivalent electrical circuit model based on charges redistribution by diffusion," *J. Power Sources*, vol. 286, pp. 58–65, Jul. 2015.
[139] A. Nadeau, M. Hassanalieragh, G. Sharma, and T. Soyata, "Energy awareness for supercapacitors using Kalman filter state-of-charge tracking," *J. Power Sources*, vol. 296, pp. 383–391, Nov. 2015.
[140] Y. Parvini, J. B. Siegel, A. G. Stefanopoulou, and A. Vahidi, "Supercapacitor electrical and thermal modeling, identification, and validation for a wide range of temperature and power applications," *IEEE Trans. Ind. Electron.*, vol. 63, no. 3, pp. 1574–1585, Mar. 2016.
[141] D. Torregrossa, M. Bahramipanah, E. Namor, R. Cherkaoui, and M. Paolone, "Improvement of dynamic modeling of supercapacitor by residual charge effect estimation," *IEEE Trans. Ind. Electron.*, vol. 61, no. 3, pp. 1345–1354, Mar. 2014.
[142] O. Bohlen, J. Kowal, and D. U. Sauer, "Ageing behaviour of electrochemical double layer capacitors: Part I. Experimental study and ageing model," *J. Power Sources*, vol. 172, no. 1, pp. 468–475, Oct. 2007.
[143] R. Chaari, O. Briat, and J.-M. Vinassa, "Capacitance recovery analysis and modelling of supercapacitors during cycling ageing tests," *Energy Convers. Manage.*, vol. 82, pp. 37–45, Jun. 2014.
[144] R. German, A. Sari, P. Venet, O. Briat, and J.-M. Vinassa, "Study on specific effects of high frequency ripple currents and temperature on supercapacitors ageing," *Microelectron. Rel.*, vol. 55, nos. 9–10, pp. 2027–2031, 2015.
[145] D. Torregrossa and M. Paolone, "Modelling of current and temperature effects on supercapacitors ageing. Part I: Review of driving phenomenology," *J. Energy Storage*, vol. 5, pp. 85–94, Feb. 2016.
[146] D. Torregrossa and M. Paolone, "Modelling of current and temperature effects on supercapacitors ageing. Part II: State-of-health assessment," *J. Energy Storage*, vol. 5, pp. 95–101, Feb. 2016.
[147] R. Kötz, M. Hahn, and R. Gallay, "Temperature behavior and impedance fundamentals of supercapacitors," *J. Power Sources*, vol. 154, no. 2, pp. 550–555, 2006.
[148] P. Guillemet, Y. Scudeller, and T. Brousse, "Multi-level reduced-order thermal modeling of electrochemical capacitors," *J. Power Sources*, vol. 157, no. 1, pp. 630–640, 2006.
[149] O. Bohlen, J. Kowal, and D. U. Sauer, "Ageing behaviour of electrochemical double layer capacitors: Part II. Lifetime simulation model for dynamic applications," *J. Power Sources*, vol. 173, no. 1, pp. 626–632, 2007.
[150] H. Gualous, H. Chaoui, and R. Gallay, "Supercapacitor calendar aging for telecommunication applications," in *Proc. IEEE Int. Telecommun. Energy Conf. (INTELEC)*, Oct. 2016, pp. 1–5.
[151] J. Schiffer, D. Linzen, and D. U. Sauer, "Heat generation in double layer capacitors," *J. Power Sources*, vol. 160, no. 1, pp. 765–772, 2006.
[152] M. Janssen and R. van Roij, "Reversible heating in electric double layer capacitors," *Phys. Rev. Lett.*, vol. 118, Mar. 2017, Art. no. 096001.
[153] A. D'Entremont and L. Pilon, "First-principles thermal modeling of electric double layer capacitors under constant-current cycling," *J. Power Sources*, vol. 246, pp. 887–898, 2014.
[154] H. Gualous, H. Louahlia-Gualous, R. Gallay, and A. Miraoui, "Supercapacitor thermal modeling and characterization in transient state for industrial applications," *IEEE Trans. Ind. Appl.*, vol. 45, no. 3, pp. 1035–1044, May 2009.
[155] H. Gualous, H. Louahlia, and R. Gallay, "Supercapacitor characterization and thermal modelling with reversible and irreversible heat effect," *IEEE Trans. Power Electron.*, vol. 26, no. 11, pp. 3402–3409, Nov. 2011.
[156] V. Lystianingrum, B. Hredzak, V. G. Agelidis, and V. S. Djanali, "On estimating instantaneous temperature of a supercapacitor string using an observer based on experimentally validated lumped thermal model," *IEEE Trans. Energy Convers.*, vol. 30, no. 4, pp. 1438–1448, Dec. 2015.
[157] I. Voicu, H. Louahlia, H. Gualous, and R. Gallay, "Thermal management and forced air-cooling of supercapacitors stack," *Appl. Therm. Eng.*, vol. 85, pp. 89–99, Jun. 2015.
[158] *LS Ultracapacitor*. Accessed: Dec. 2018. [Online]. Available: http://www.ultracapacitor.co.kr/?enc=L3N1Yi9wcm9kdWN0L3N1YjFfMS5odG1s
[159] Nesscap Products. *Nesscap Ultracapacitors*. Accessed: Sep. 2018. [Online]. Available: http://www.nesscap.com/product/p_overview.jsp
[160] Panasonic Corp. *Electric Double Layer Capacitors (Gold Capacitors)*. Accessed: Jan. 2019. [Online]. Available: https://industrial.panasonic.com/ww/products/capacitors/edlc
[161] Ioxus. *Products Overview*. Accessed: Feb. 2019. [Online]. Available: http://www.ioxus.com/english/products/
[162] Sps cap. *Supreme Power Solutions*. Accessed: Jan. 2019. [Online]. Available: http://spscap.com/en/
[163] N. Blomquist, T. Wells, B. Andres, J. Bäckström, S. Forsberg, and H. Olin, "Metal-free supercapacitor with aqueous electrolyte and low-cost carbon materials," *Sci. Rep.*, vol. 7, Jan. 2017, Art. no. 39836.
[164] B. C. Kim, J.-Y. Hong, G. G. Wallace, and H. S. Park, "Recent progress in flexible electrochemical capacitors: Electrode materials, device configuration, and functions," *Adv. Energy Mater.*, vol. 5, no. 22, 2015, Art. no. 1500959.
[165] M. Yousaf *et al.*, "Novel pliable electrodes for flexible electrochemical energy storage devices: Recent progress and challenges," *Adv. Energy Mater.*, vol. 6, no. 17, 2016, Art. no. 1600490.
[166] H. Li *et al.*, "Flexible all-solid-state supercapacitors with high volumetric capacitances boosted by solution processable MXene and electrochemically exfoliated graphene," *Adv. Energy Mater.*, vol. 7, no. 4, 2017, Art. no. 1601847.
[167] Y. Guo, W. Li, H. Yu, D. F. Perepichka, and H. Meng, "Flexible asymmetric supercapacitors via spray coating of a new electrochromic donor–acceptor polymer," *Adv. Energy Mater.*, vol. 7, no. 2, 2017, Art. no. 1601623.
[168] A. Scalia *et al.*, "A flexible and portable powerpack by solid-state supercapacitor and dye-sensitized solar cell integration," *J. Power Sources*, vol. 359, pp. 311–321, Aug. 2017.
[169] J. Rinne, J. Keskinen, P. R. Berger, D. Lupo, and M. Valkama, "Viability bounds of M2M communication using energy-harvesting and passive wake-up radio," *IEEE Access*, vol. 5, pp. 27868–27878, 2017.
[170] Adif. *Ferrolinera Project*. Accessed: Feb. 2019. [Online]. Available: http://www.adif.es/es_ES/comunicacion_y_prensa/fichas_de_actualidad/ficha_actualidad_00072.shtml
[171] Siemens AG. *Sitras SES: Stationary Energy Storage System for DC Traction Power Supply*. Accessed: Feb. 2019. [Online]. Available: https://w3.usa.siemens.com/mobility/us/Documents/en/rail-solutions/railway-electrification/dc-traction-power-supply/sitras-ses-en.pdf
[172] *Ultracapacitors: Transforming the Grid*, Maxwell Technol., San Diego, CA, USA, 2015.
[173] F. Ciccarelli, A. Del Pizzo, and D. Iannuzzi, "Improvement of energy efficiency in light railway vehicles based on power management control of wayside lithium-ion capacitor storage," *IEEE Trans. Power Electron.*, vol. 29, no. 1, pp. 275–286, Jan. 2014.
[174] H. Li, J. Peng, J. He, R. Zhou, Z. Huang, and J. Pan, "A cooperative charging protocol for onboard supercapacitors of catenary-free trams," *IEEE Trans. Control Syst. Technol.*, vol. 26, no. 4, pp. 1219–1232, Jul. 2018.
[175] L. P. Di Noia, F. Genduso, R. Miceli, and R. Rizzo, "Optimal integration of hybrid supercapacitor and IPT system for a free-catenary tramway," *IEEE Trans. Ind. Appl.*, vol. 55, no. 1, pp. 794–801, Jan. 2019.
[176] Z. Song, H. Hofmann, J. Li, J. Hou, X. Han, and M. Ouyang, "Energy management strategies comparison for electric vehicles with hybrid energy storage system," *Appl. Energy*, vol. 134, pp. 321–331, Dec. 2014.
[177] Z. Song, J. Hou, S. Xu, M. Ouyang, and J. Li, "The influence of driving cycle characteristics on the integrated optimization of hybrid energy storage system for electric city buses," *Energy*, vol. 135, pp. 91–100, Sep. 2017.

[178] A. Burke and H. Zhao, "Applications of supercapacitors in electric and hybrid vehicles," in *Proc. 5th Eur. Symp. Supercapacitor Hybrid Solutions (ESSCAP)*, Brasov, Romania, 2015, pp. 1–15.

[179] Mazda. *i-ELOOP Capacitor-Based Brake Energy Regeneration System*. Accessed: Feb. 2019. [Online]. Available: http://www2.mazda.com/en/publicity/release/2011/201111/111125a.html

[180] Y. Maletin *et al.*, "New approach to ultracapacitor technology: What it can offer to electrified vehicles," *J. Energy Power Eng.*, vol. 9, no. 6, pp. 585–591, 2015.

[181] M. Ouyang *et al.*, "Performance analysis of a novel coaxial power-split hybrid powertrain using a CNG engine and supercapacitors," *Appl. Energy*, vol. 157, pp. 595–606, Nov. 2015.

[182] J. Trovão and C. Antunes, "A comparative analysis of meta-heuristic methods for power management of a dual energy storage system for electric vehicles," *Energy Convers. Manage.*, vol. 95, pp. 281–296, May 2015.

[183] A. Castaings, W. Lhomme, R. Trigui, and A. Bouscayrol, "Comparison of energy management strategies of a battery/supercapacitors system for electric vehicle under real-time constraints," *Appl. Energy*, vol. 163, pp. 190–200, Feb. 2016.

[184] D. Rezzak and N. Boudjerda, "Management and control strategy of a hybrid energy source fuel cell/supercapacitor in electric vehicles," *Int. Trans. Elect. Energy Syst.*, vol. 27, no. 6, p. e2308, 2017.

[185] M. G. Carignano, R. Costa-Castelló, V. Roda, N. M. Nigro, S. Junco, and D. Feroldi, "Energy management strategy for fuel cell-supercapacitor hybrid vehicles based on prediction of energy demand," *J. Power Sources*, vol. 360, pp. 419–433, Aug. 2017.

[186] R. German, A. Hammar, R. Lallemand, A. Sari, and P. Venet, "Novel experimental identification method for a supercapacitor multipore model in order to monitor the state of health," *IEEE Trans. Power Electron.*, vol. 31, no. 1, pp. 548–559, Jan. 2016.

[187] S. N. Motapon, L.-A. Dessaint, and K. Al-Haddad, "A comparative study of energy management schemes for a fuel-cell hybrid emergency power system of more-electric aircraft," *IEEE Trans. Ind. Electron.*, vol. 61, no. 3, pp. 1320–1334, Mar. 2014.

[188] I. Egido *et al.*. "A comprehensive research and demostration project on the application of energy storage systems in island power systems," *CIGRE Session*, vol. 46, Aug. 2016, Art. no. 135990

[189] N. P. Brandon *et al.*, "UK research needs in grid scale energy storage technologies," Energy Storage Res. Netw. Eng. Phys. Sci. Res. Council, London, U.K., White Paper, 2016.

[190] S. Werkstetter, "Ultracapacitor usage in wind turbine pitch control systems," Maxwell Technol., San Diego, CA, USA, Tech. Rep. 3000722, 2015.

[191] G. Ren, J. Liu, J. Wan, Y. Guo, and D. Yu, "Overview of wind power intermittency: Impacts, measurements, and mitigation solutions," *Appl. Energy*, vol. 204, pp. 47–65, Oct. 2017.

[192] A. Abedini and A. Nasiri, "Applications of super capacitors for PMSG wind turbine power smoothing," in *Proc. 34th Annu. Conf. IEEE Ind. Electron.*, Nov. 2008, pp. 3347–3351.

[193] L. Qu and W. Qiao, "Constant power control of DFIG wind turbines with supercapacitor energy storage," *IEEE Trans. Ind. Appl.*, vol. 47, no. 1, pp. 359–367, Jan. 2011.

[194] W. Li, G. Joos, and J. Belanger, "Real-time simulation of a wind turbine generator coupled with a battery supercapacitor energy storage system," *IEEE Trans. Ind. Electron.*, vol. 57, no. 4, pp. 1137–1145, Apr. 2010.

[195] H. Zhao and W. Guo, "Hierarchical distributed coordinated control strategy for hybrid energy storage array system," *IEEE Access*, vol. 7, pp. 2364–2375, 2019.

[196] X. Wang, K. W. E. Cheng, and Y. C. Fong, "Series-parallel switched-capacitor balancing circuit for hybrid source package," *IEEE Access*, vol. 6, pp. 34254–34261, 2018.

[197] J. Pegueroles-Queralt, F. D. Bianchi, and O. Gomis-Bellmunt, "A power smoothing system based on supercapacitors for renewable distributed generation," *IEEE Trans. Ind. Electron.*, vol. 62, no. 1, pp. 343–350, Jan. 2015.

[198] F. Bensmaine, O. Bachelier, S. Tnani, G. Champenois, and E. Mouni, "LMI approach of state-feedback controller design for a STATCOM-supercapacitors energy storage system associated with a wind generation," *Energy Convers. Manage.*, vol. 96, pp. 463–472, May 2015.

[199] I. de la Parra, J. Marcos, M. García, and L. Marroyo, "Improvement of a control strategy for PV power ramp-rate limitation using the inverters: Reduction of the associated energy losses," *Sol. Energy*, vol. 127, pp. 262–268, Apr. 2016.

[200] Y. Kim, V. Raghunathan, and A. Raghunathan, "Design and management of battery-supercapacitor hybrid electrical energy storage systems for regulation services," *IEEE Trans. Multi-Scale Comput. Syst.*, vol. 3, no. 1, pp. 12–24, Jan. 2017.

[201] U. Akram and M. Khalid, "A coordinated frequency regulation framework based on hybrid battery-ultracapacitor energy storage technologies," *IEEE Access*, vol. 6, pp. 7310–7320, 2018.

[202] J. Pascual, J. Barricarte, P. Sanchis, and L. Marroyo, "Energy management strategy for a renewable-based residential microgrid with generation and demand forecasting," *Appl. Energy*, vol. 158, pp. 12–25, Nov. 2015.

[203] A. Berrueta, M. Heck, M. Jantsch, and A. Ursúa, and P. Sanchis, "Combined dynamic programming and region-elimination technique algorithm for optimal sizing and management of lithium-ion batteries for photovoltaic plants," *Appl. Energy*, vol. 228, pp. 1–11, Oct. 2018.

[204] X. Lu, Y. Chen, M. Fu, and H. Wang, "Multi-objective optimization based real-time control strategy for battery/ultracapacitor hybrid energy management systems," *IEEE Access*, to be published.

[205] H. F. Habib, M. El Hariri, A. Elsayed, and O. A. Mohammed, "Utilization of supercapacitors in protection schemes for resiliency against communication outages: A case study on size and cost optimization," *IEEE Trans. Ind. Appl.*, vol. 54, no. 4, pp. 3153–3164, Jul. 2018.

[206] H. Camblong, S. Baudoin, I. Vechiu, and A. Etxeberria, "Design of a SOFC/GT/SCs hybrid power system to supply a rural isolated microgrid," *Energy Convers. Manage.*, vol. 117, pp. 12–20, Jun. 2016.

[207] S. Wen, S. Wang, G. Liu, and R. Liu, "Energy management and coordinated control strategy of PV/HESS AC microgrid during Islanded operation," *IEEE Access*, vol. 7, pp. 4432–4441, 2019.

[208] S. Kotra and M. K. Mishra, "A supervisory power management system for a hybrid microgrid with HESS," *IEEE Trans. Ind. Electron.*, vol. 64, no. 5, pp. 3640–3649, May 2017.

[209] U. Akram, M. Khalid, and S. Shafiq, "An innovative hybrid wind-solar and battery-supercapacitor microgrid system—Development and optimization," *IEEE Access*, vol. 5, pp. 25897–25912, 2017.

[210] I. S. Martín, A. Ursúa, and P. Sanchis, "Integration of fuel cells and supercapacitors in electrical microgrids: Analysis, modelling and experimental validation," *Int. J. Hydrogen Energy*, vol. 38, no. 27, pp. 11655–11671, 2013.

[211] R. Ferrero, M. Marracci, and B. Tellini, "Single PEM fuel cell analysis for the evaluation of current ripple effects," *IEEE Trans. Instrum. Meas.*, vol. 62, no. 5, pp. 1058–1064, May 2013.

[212] M. Gerard, J.-P. Poirot-Crouvezier, D. Hissel, and M.-C. Péra, "Ripple current effects on PEMFC aging test by experimental and modeling," *J. Fuel Cell Sci. Technol.*, vol. 8, no. 2, 2010, Art. no. 021004.

[213] M. Jung and K. A. Williams, "Effect of dynamic operation on chemical degradation of a polymer electrolyte membrane fuel cell," *J. Power Sources*, vol. 196, no. 5, pp. 2717–2724, 2011.

[214] M. Yoshida, Y. Tsukamoto, T. Matsuda, Y. Dougan, and K. Ueno, "Introducing electric-powered forklift truck 'New ARION' series," Komatsu, Tokyo, Japan, Tech. Rep. 214, 2007.

[215] M. Conte, A. Genovese, F. Ortenzi, and F. Vellucci, "Hybrid battery-supercapacitor storage for an electric forklift: A life-cycle cost assessment," *J. Appl. Electrochem.*, vol. 44, no. 4, pp. 523–532, 2014.

[216] N. Zhao, N. Schofield, and W. Niu, "Energy storage system for a port crane hybrid power-train," *IEEE Trans. Transp. Electrific.*, vol. 2, no. 4, pp. 480–492, Dec. 2016.

[217] Komatsu. *Introduces the World's First Hydraulic Excavator: Hybrid Evolution Plan for Construction Equipment*. Accessed: Feb. 2019. [Online]. Available: http://www.komatsu.com/CompanyInfo/press/2008051315113604588.html

[218] Caterpillar. *Caterpillar Announces Development of Largest Hydraulic Shovel*. Accessed: Jan. 2019. [Online]. Available: http://www.cat.com/en_GB/news/machine-press-releases/caterpillar-announcesdevelopmentoflargesthydraulicshovel.html

[219] Rockster Recycler. *A Revolutionary New Technology*. Accessed: Apr. 2019. [Online]. Available: https://www.rockster.at/content/en/aktuelles-news/fortschritt_durch_neue_technologie_rocksters_neuer_hybrid_prallbrecher_setzt_neue_massstaebe

[220] P. Mars, "Supercapacitors for SSD backup power," *Electron. Products*, vol. 51, no. 10, pp. 40–41, 2009.

[221] M. Helmlinger, "Supercapacitor backup power supply with active cell balancing," Texas Instrum., Dallas, TX, USA, Tech. Rep. PMP9766, 2015.

[222] J. R. Miller, "Engineering electrochemical capacitor applications," *J. Power Sources*, vol. 326, pp. 726–735, Sep. 2016.

[223] M. Hassanalieragh, T. Soyata, A. Nadeau, and G. Sharma, "UR-SolarCap: An open source intelligent auto-wakeup solar energy harvesting system for supercapacitor-based energy buffering," *IEEE Access*, vol. 4, pp. 542–557, 2016.
[224] STMicroelectronics. *STMicroelectronics Breaks Through LED Camera Flash Limitations*. Accessed: Feb. 2019. [Online]. Available: http://www.cap-xx.com/wp-content/uploads/2015/04/ST-Microelectronics-Breaks-through-LED-Camera-Flash-Limitations.pdf

ALBERTO BERRUETA (S'15–M'18) was born in Pamplona, Spain, in 1989. He received the Ph.D. degree in electrical engineering from the Public University of Navarre, Pamplona, in 2017, where he is currently a Researcher and a Lecturer. In 2013, he joined the Electrical Engineering, Power Electronics, and Renewable Energy Research Group, Public University of Navarre, where he has been with the Research Institute of Smart Cities, since 2015. His research interests include electrochemical modeling, thermal performance, and aging of lithium-ion batteries and supercapacitors.

ALFREDO URSÚA (M'04) received the B.Sc. and M.Sc. degrees (Hons.) in electrical engineering and the Ph.D. degree in electrical engineering from the Public University of Navarre, Spain, in 2001, 2004, and 2010, respectively.

In 2002, he joined the Department of Electrical, Electronic, and Communications Engineering, Public University of Navarre, where he is currently an Associate Professor. He is also the Vice Dean of the School of Industrial and ICT Engineering and a member of the Steering Committee of the University Chair for Renewable Energies. He has been involved in several research projects both with private and public funding and mainly related to renewable energy systems, electric energy storage technologies, power electronics, energy management, and electric microgrids. He has coauthored more than 60 journal papers and conference contributions and supervised three Ph.D. theses. He holds two patents. He is a member of the Spanish Hydrogen Association.

IDOIA SAN MARTÍN received the M.Sc. degree in electrical engineering, the M.Sc. degree in renewable energies, and the Ph.D. degree from the Public University of Navarre, Spain, in 2007, 2009, and 2013, respectively, where she joined the Electrical Engineering, Power Electronics, and Renewable Energy Research Group, in 2007, and is currently an Associate Professor with the Department of Electrical, Electronic, and Communications Engineering and the Technical Secretary of the Renewable Energies Chair. She has been with the Research Institute of Smart Cities, the Public University of Navarre, since 2015. Her research is focused on the analysis of energy storage systems to improve the grid integration of renewable energies, with a special attention to supercapacitors, lead acid batteries, lithium-ion batteries, and hydrogen systems.

ALI EFTEKHARI is currently a Professor of chemistry with the Belfast Academy. He has worked in different capacities in various universities across four continents and founded two internationally recognized academic schools from scratch, which were considered as exceptional success stories by major media, such as British newspaper, The Guardian. He is the Principal Author of over 100 papers published in leading scholarly journals and has supervised over 110 postdoctoral researchers and graduate students. His research interest is focused on the material design for electrochemical systems and has involved in energy storage systems for 20 years. He is the President of the American Nano Society.

PABLO SANCHIS (M'03–SM'12) received the M.Sc. and Ph.D. degrees in electrical engineering and the M.Sc. degree in management and business administration from the Public University of Navarre, Pamplona, Spain, in 1995, 2002, and 1994, respectively.

From 1996 to 1998, he was a Guest Researcher with the Delft University of Technology, The Netherlands. In 1998, he joined the Department of Electrical, Electronic, and Communications Engineering, Public University of Navarre (UPNA), where he is currently an Associate Professor. He was the Vice Dean of the School of Industrial and Telecommunications Engineering. He is also the Director of the UPNA Chair for Renewable Energies and the Director of the Research Resources and Structures Unit, UPNA. He has been involved in more than 70 research projects both with public funding and in co-operation with industry. He has also coauthored more than 140 papers and contributions in international journals and conferences and has supervised nine Ph.D. thesis. He is the Co-Inventor of eight patents. He received the UPNA Research Award for the best technical paper, in 2013, and the UPNA Excellence in Teaching Award, in 2017. His research interests include renewable energies, power electronics, electric energy storage technologies, grid integration of renewable energies, and electric microgrids.